CRACKING POTENTIAL OF SHORT- AND LONG-TERM AGED BINDER WITH VARIOUS LEVELS OF ABR

BY

JING MA

THESIS

Submitted in partial fulfillment of the requirements
for the degree of Master of Science in Civil Engineering
in the Graduate College of the
University of Illinois at Urbana-Champaign, 2017

Urbana, Illinois

Advisers:

Professor Imad L. Al-Qadi
Research Assistant Professor Hasan Ozer

ABSTRACT

It is widely accepted that using reclaimed asphalt pavement (RAP) and recycled asphalt shingles (RAS) could improve the sustainability of asphalt concrete (AC), in terms of cost savings and environmental factors. This should be only valid when short- and long-term pavement performance are not compromised. This thesis presents an experimental evaluation of the rheological properties of binders from various sources to investigate the effects of aging and increasing asphalt binder replacement (ABR) levels. In addition to the standard Superpave grading parameters, the additional rheological parameters for low-temperature cracking susceptibility and block and fatigue cracking were derived from various dynamic shear rheometer (DSR) and bending beam rheometer (BBR) tests. Binders from five AC designed with varying ABR percentages (from 0 to 60%) were recovered using the standard Rotovap test procedure. The base binder used in the AC design and binders recovered from RAP and RAS were also tested. In addition to standard aging protocols, base binders were subjected to a second pressure aging vessel (PAV), while one PAV was applied for the extracted binders. Almost all additional rheological parameters appeared to maintain consistent trends with aging and increasing ABR levels. The considered parameters are shown to be helpful in evaluating progression in the brittleness of binders with ABR and aging. Based on the outcome of the experimental program (binder level and mixture level), it was concluded that AC with ABR levels above 20 percent could suffer from short- and long-term cracking potential. Asphalt concrete with high ABR content can already be at a critically-aged condition immediately after production and, as a result, aging progresses much faster in the binders of such mixes.

ACKNOWLEDGEMENTS

I would first like to thank my advisor, Professor Imad Al-Qadi, for providing me such a great opportunity to be a graduate research assistant. It has been a privilege to learn from Professor Al-Qadi and to benefit from his professional expertise.

Also I feel very fortunate to work with Professor Hasan Ozer. This thesis would not have been possible without his guidance and invaluable advice.

This study is based on the results of Project No. ICT-R27-162, Modeling the Performance Properties of RAS Blended Asphalt Mixes Through Chemical Compositional Information. ICT-R27-162 was conducted in cooperation with the Illinois Center for Transportation and the Illinois Department of Transportation. I would like to acknowledge all the staff and students at the Illinois Center for Transportation; thanks for giving me the test training and helping me with various testing protocols.

Finally, a special thanks to my family members and all my friends for their companionship and encouragement.

TABLE OF CONTENTS

CHAPTER 1 INTRODUCTION

It is widely accepted that using reclaimed asphalt pavement (RAP) and recycled asphalt shingles (RAS) could improve the sustainability of asphalt concrete (AC), in terms of cost savings and environmental factors, when short- and long-term pavement performance is not compromised. In the state of Illinois and elsewhere in the United States, various type of recycled and waste materials were utilized in highway construction. There are numerous studies in the literature on the use of reclaimed and recycled materials used in Illinois highway construction (Liu et al.2015; Rowden et al. 2012; Lippert et al. 2012). In recent years, reclaimed asphalt shingles (RAS) have also been introduced as a recycled material containing significantly high petroleum based binder (20-30% by weight). The use of RAP and RAS together led to increase amount of virgin asphalt binder replacement. Using RAP and RAS provides numerous economic benefits primarily because it serves as a replacement for petroleum-based asphalt binder. On the other hand, as asphalt binder replacement (ABR) levels increase, arise the difficulties in the production and in-service performance of pavements built with such mixes. For example, reclaimed asphalt materials introduce aged and brittle asphalts into the pavement, which may influence AC performance during cold weather. To counter these hard asphalts, softer asphalts are often incorporated into the AC. The goal for the final mix is to obtain properties suitable to achieve the desired design lifetime of the pavement. Therefore, a thorough study was conducted to evaluate the rheology performance of a blend of RAS, RAP, and virgin binders used in highway construction.

1. 1 Problem Statement

There are various challenges and performance risks associated with the use of RAP and RAS. Recycled binder used in RAP and RAS is often considerably more aged than virgin binder (AASHTO, 2014). The increased stiffness associated with aging can pose premature cracking risks in the field, the rutting resistance of AC may improve on the other hand (Cooper et al. 2015). A second challenge is the variability in aggregate and binder properties of RAP stockpiles. Finally, unknown or partial blending of recycled binder with the original binder could result with insufficient total binder content in the AC mix. Partial blending can influence AC's compaction, and hence hinder the achievement of target density in the field. In additional, partial blending may result in the heterogeneous distribution of recycled binder in the AC mixes.

Many studies have investigated the effect of increased levels of RAP and RAS on the characteristics of AC and binders (Cascione et al. 2015; Chen et al. 2014; Daniel et al. 2010). A comprehensive summary of literature on the effects of RAP and RAS or asphalt binder replacement (ABR) on AC performance characteristics was conducted by Li and Gibson (2012). At the AC level, most of these studies concluded that low-temperature and fatigue cracking of AC with high ABR material could be increased due to the AC brittleness (Mensching et al. 2015). Depending on the test methods and quality of laboratory AC design preparation and specimen fabrication, the significance of the impact varied, and the results were inconsistent. However, the majority of the studies demonstrated an improvement in rutting resistance of AC with increasing recycled content. In most of the available studies, AC characterization with recycled content was limited to short-term-aged, laboratory-produced, and plant-produced AC mixes.

Even though AC performance tests can have a direct relationship with field performance of pavements, binder characterization has also been considered when evaluating the effects of recycled binder, modifiers, and additives at the constituent level. Some of the standard binder tests include intermediate- and high-temperature dynamic shear rheometer (DSR) and low-temperature bending beam rheometer (BBR) tests. In Colbert et al. (2012), virgin binder was blended with 30%, 50%, 70%, and 100% RAP binder before evaluation by aging: rolling thin-film oven (RTFO) aging, and pressure aging vessel (PAV) aging. The study found that the higher the viscosity of binder blends the greater increase of stiffness after aging (Colbert et al. 2012). Other studies showed that standard Superpave tests might not accurately and consistently capture the intermediate-temperature behavior of binders, especially when they are blended with modifiers or recycled content (Abbas et al. 2013; Gibson et al. 2012; Huang et al. 2014; Khosla et al. 2012; Zhou et al. 2013). Additional test methods and analysis approaches were proposed to characterize the AC cracking susceptibility in the presence of modifiers, additives, and recycled content under standard and extreme conditions. Beyond Superpave standard tests, Gibson et al. (2012) used full scale with accelerated pavement test (APT) to compare the fatigue cracking susceptibility of binder with various polymer modifiers. The results indicated that critical tip opening displacement (CTOD) and binder yield energy had more discrimination potential than did the Superpave parameters.

Recently, several other binder performance criteria have been developed. One developed by Rowe (2014) can be used for predicting fatigue and block cracking susceptibility of binders at intermediate temperatures. The parameter is derived from DSR complex modulus tests and is known as the Glover-Rowe (GR) parameter. The R-value and crossover frequency are additional parameters that can be obtained from DSR temperature and frequency-sweep tests. As for low-temperature performance, a new parameter, ΔT_c , defined as the difference between critical temperature of stiffness and m-value obtained from the BBR test, where stiffness threshold equals 300 MPa and the m-value is 0.300 (King et al. 2012). These parameters were recently utilized by Mogawer et al. (2016) to assess the impact of re-refined engine oil bottoms (ReOB) using two different binder grades and various aging durations. The parameters showed the progression of brittleness with aging for the two ReOB sources when compared with control binders.

The aforementioned studies emphasize the need for reliable AC and binder performance test methods and the need for criteria to evaluate AC containing high recycled content or binders. Because the performance of blended binders and AC with recycled content after long-term aging has not been clearly understood, limits were generally determined based on engineering judgment or plant production capacity rather than using experimental characterization, supported with field results.

1.2 Research Objectives

The main goal of this study is to evaluate various binder performance criteria in relation to cracking susceptibility of binders with recycled content, including RAP and RAS. Some of the specific objectives of study are summarized below:

- Characterize the short- and long-term rheological properties of the extracted binders containing RAP and RAS using standard Superpave and non-standard, recently-developed methods and criteria;
- Evaluate various binder performance criteria for effectively and consistently characterizing the effects of ABR and aging;
- Assess aging history and progression with binders containing various percentages of RAP and RAS;

- Propose critical thresholds of ABR above which the binder and AC mixture's cracking potential could be increased at which point remediation should be considered.

1.3 Research Approach

This thesis presents the results of an experimental program developed to characterize short- and long-term performance of binders with various levels of RAP and RAS binder content. Binders from five AC designed with varying ABR percentages (0 to 60%) were recovered using the standard Rotovap test procedure. A proven aging method exists to evaluate the long-term impact of recycled materials (Colbert et al. 2012). In addition to standard aging protocols, base binders were subjected to a second pressure aging vessel (PAV), while one PAV was applied for the extracted binders in order to simulate long-term performance. Also, beyond the standard Superpave grading parameters, the additional rheological parameters for low-temperature cracking susceptibility and block and fatigue cracking potential were derived from various DSR and BBR tests. Binder performance tests were chosen in this study because they offer several advantages. Test results of binders are more repeatable because of the relatively homogenous microstructure of binders compared with that of AC. The effect of changes in the constituents (e.g., the addition of recycled binder at different ratios or modifiers) can directly affect the results.

1.4 Thesis Organization

The introduction of this thesis gives a description of the problem statement, research objectives, and research approach. Chapter 2 covers related test methods and some new rheology parameters used in this study, in addition to a detailed literature review. Chapter 3 presents materials used and the test considered in this study, such as the equipment setting parameters (frequency, temperature, etc.), and the number of replicates used in each test. The results are discussed in Chapter 4, while Chapter 5 presents the study conclusions and offers some recommendations for future work.

CHAPTER 2 CURRENT STATE OF KNOWLEDGE

This chapter presents a comprehensive review of the conventional and more recent and advanced rheological test methods employed for characterization of asphalt binder. Test methods will be introduced along with typical results.

2.1 Related Test Methods

2.1.1 Binder Recovery

In this study, the binder recovery from the AC mixtures followed the AASHTO T391-15, "Standard Method of Test for Quantitative Extraction and Recovery of Asphalt Binder from Asphalt Mixtures." Following the specifications, the AC mixture was repeatedly washed and filtered with solvent (Entron used in this study) in a filtration apparatus. Each filtration was then distilled under vacuum in a rotary evaporator with the asphalt remaining in the flask (Figure 2.1). The solvent was distilled at 100°C. After recovery of the final filtrate, the solution was concentrated to about 300 mL and centrifuged to remove the aggregate fines. At the final phase when the nitrogen gas introduced, the distillation temperature was increased to 174°C.

Figure 2.1 Rotovap binder recovery equipment

2.1.2 Aging Methods

In order to evaluate short- and long-term binder performance, two aging methods were used. The Rolling Thin Film Oven (RTFO) was used to simulate short-term aging and the Pressure Aging Vessel (PAV) was used to simulate long-term aging.

2.1.2.1 Rolling Thin Film Oven (RTFO)

RTFO aging is a short-term aging method that represents aging performance during construction. In accordance with ASTM D2872, the asphalt material should be heated in the RTFO for 85 min at 163°C under air pressure. The machine can hold eight bottles at a time (Figure 2.2). The mass of the material in each bottle should be 35 ± 0.5 g, and the mass change of each bottle after aging should be less than 1%. In this study, RTFO aged material was used to conduct the DSR tests and PAV tests.

Figure 2.2 RTFO aging equipment

2.1.2.2 Pressure Aging Vessel (PAV)

The PAV aging method simulates long-term aging conditions of asphalt binder. This test needs to be conducted on the standard RTFO aged residue. The basic procedure starts with pouring the heated RTFO aged binder into the PAV pans. Each pan can contain up to 50 g material, and ten pans can be heated at one time. The whole aging process takes 20 hrs under 305 psi air pressure. In this study, the PAV aged material was used in both DSR and BBR tests.

Figure 2.3 PAV aging equipment

2.1.3 Rheology Testing Method

The two main rheology tests used in this study to characterize the binder performance are the DSR and BBR tests. Following the ASTM D6373 Superpave PG grading, the DSR should be conducted on both RTFO aged binder at high temperature and PAV aged binder at intermediate temperature, while the BBR test should conducted on the PAV aged binder at low temperature.

2.1.3.1 Dynamic Shear Rheometer (DSR)

The DSR is used to characterize the viscous and elastic behavior of asphalt binders at intermediate and high temperatures. The basic DSR test uses a thin asphalt binder sample sandwiched between two circular parallel plates. The lower plate is fixed, while the upper plate oscillates back and forth across the sample to create a shearing action. The frequency can be changed or fixed and the test temperature can be controlled. Figure 2.4 shows the DSR equipment used in the study.

Figure 2.4 DSR equipment

Two important parameters can be obtained from the DSR test: G^* (complex modulus) and δ (phase angle). The complex modulus is defined by the following equation, where τ_{max} is the shear stress and γ_{max} is the shear strain:

$$G^* = \frac{\tau_{max}}{\gamma_{max}} \quad (2.1)$$

δ is the lag between applied shear stress and the resulting shear strain. The phase angle presents the viscoelasticity of binder and allows obtaining the binder stress relaxation. For failure at the same stiffness level, a lower phase angle means less strain than a higher phase angle.

In this study, the Superpave high temperature grading and the frequency sweep tests were performed.

Superpave High-Temperature Grading

The test undertaken was the Superpave high-temperature grading test. This test is used to determine the high temperature Superpave PG grade of the binder. A complete high temperature grading requires two sets of grading tests. One is conducted on the un-aged binder and the other on the RTFO aged binder; both use a 25 mm sample size. According to the Superpave specifications developed by the Strategic Highway Research Program (SHRP), $G^*/\sin\delta$, defined

as the rutting parameter and the minimum limit, placed at 10 rad/sec (1.59 Hz) —for un-aged binder it was 1.0 kPa; for RTFO-aged binders it was 2.2 kPa.

In this study, the high-temperature grading tests were conducted on un-aged, RTFO-aged, and extracted un-aged binders at high temperature.

Superpave Intermediate-Temperature Grading

The DSR equipment can be used for measuring binder resistance to fatigue cracking. Based on the Superpave specification, $|G^*|\sin\delta$ is defined as the fatigue cracking parameter and with a maximum limit of 5,000 kPa, measured at a strain amplitude of 1%, and a frequency of 10 rad/sec. This test is also conducted on the PAV residue at intermediate temperature, and the sample size is 8 mm diameter with a 2 mm thickness. Results of this test are used to build a binder master curve over a wide range of temperatures or reduced frequencies.

Characterization of Linear Viscoelasticity using Master Curves

The temperature-frequency sweep test was conducted at different temperatures, and at each temperature with a range of frequencies within the linear stain range. Based on the results from this test, the master curve can be developed by shifting the curve at every temperature to a reference temperature (usually an intermediate temperature—28°C in this study). The master curve is generally a binder performance function at a constant (reference) temperature, with the x-axis of reduced frequency and the y-axis of binder (complex modulus, phase angle, etc.).

The master curve constructed as a result of temperature-frequency tests is a useful linear viscoelastic characterization method for detecting the overall performance of binder. It can provide the binder's fundamental properties (complex modulus and phase angle) versus a large range frequency by conducting the test at different temperatures, then shifting it to a same reference temperature using various models. When conducting the test, the sample size varies depending on the material hardness and test temperature. Generally, a 25 mm × 1 mm sample size was used for high temperature testing (40-90℃) and 8 mm × 2 mm was used for low and intermediate temperature testing (-5-40℃, Huang et al. 2014).

The outcome of the temperature-frequency tests is master curves defining the complex modulus G^* or phase angle δ across a wide range of temperatures and frequencies. In this study, The MEPDG Sigmoidal model is used to fit the curves. The following figures are not test results from this study, but are presented to illustrate the basic idea of time temperature superposition.

Figure 2.5 shows the direct results from frequency sweep tests; each point represents the test results at a specific temperature and frequency (linear strain range). Figure 2.6 shows that these curves can be shifted to a single curve by changing their test frequencies but not the value of the modulus—which is a master curve—and the changed frequency—which is called the reduced frequency. The strategy of changing frequency is to simply multiply each frequency with a shift factor a_T. Then, this curve can be fitted to various models; the MEPDG Sigmoidal model was used in this study.

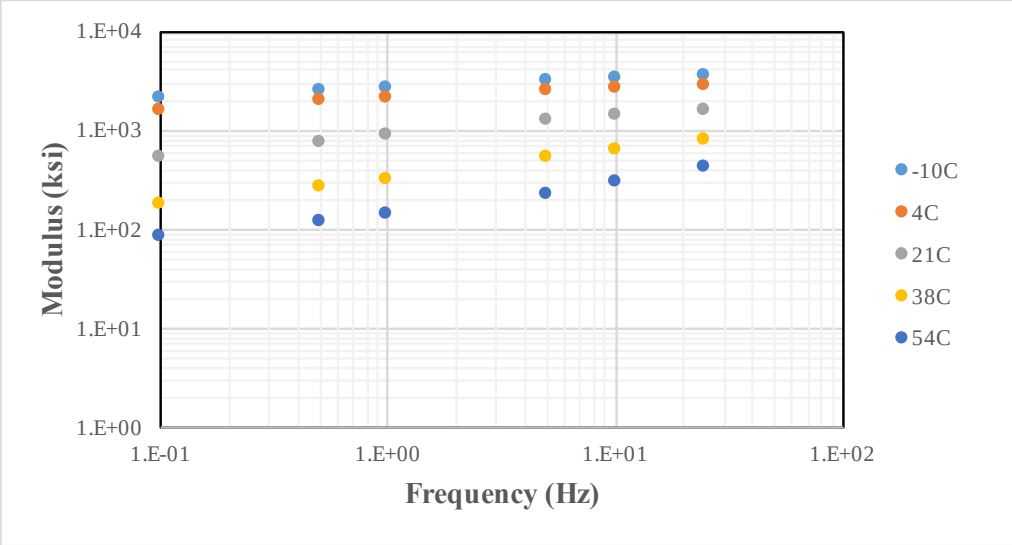

Figure 2.5 Frequency sweep test results before time-temperature superposition

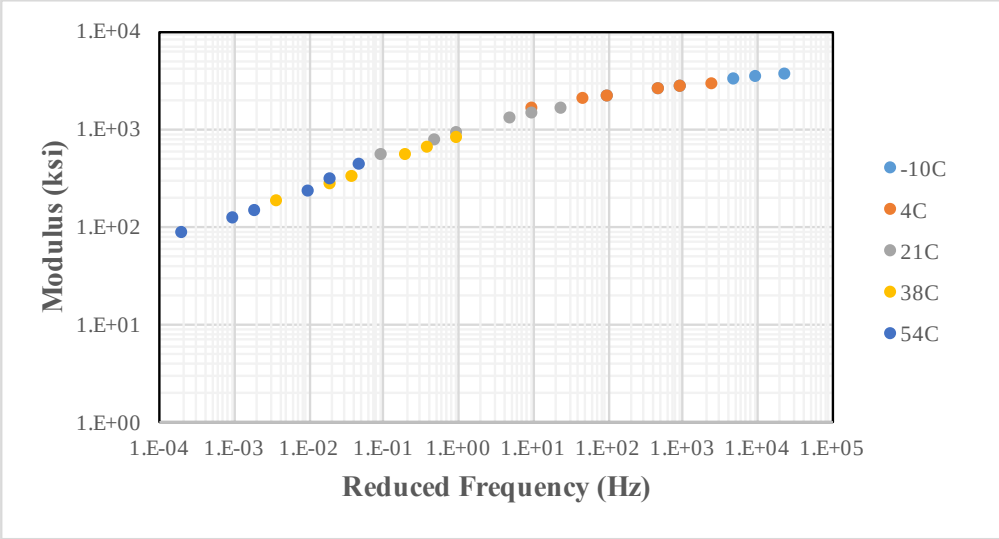

Figure 2.6 Frequency sweep test results after time-temperature superposition

The relationship between shift factor and the temperature can be described by the WLF model. The WLF equation is:

$$\log(a_T) = -C1(T - T_0)/(C2 + (T - T_0)) \quad (2.2)$$

where T_0 is the reference temperature (shift factor 0 and 28°C in this study); T is the input temperature; and $C1$ and $C2$ are fitted constants.

Based on the WLF equation, we can derive the rheology properties at any temperature and frequency. For instance, the Glover-Rowe (GR) parameter $G * (\cos\delta)^2/\sin\delta$ was measured at 15°C to be 0.005 rad/sec. We can back calculate the shift factor based on the WLF equation by inputting T = 15°C; once we know the frequency and shift factor, the reduced frequency can be easily derived. Once the reduced frequency is obtained, the complex modulus and phase angle can also be easily derived from the constructed master curves. Figure 2.7 shows an example of WLF fitting.

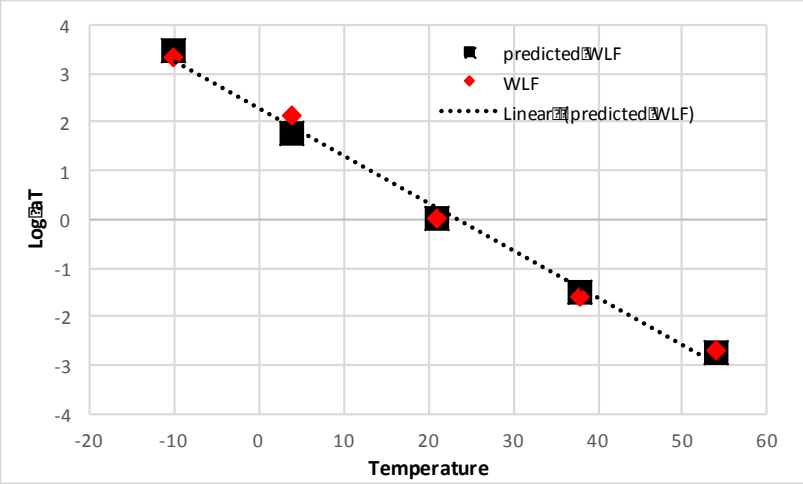

Figure 2.7 WLF model fit example

In this study, in addition to the Superpave rheology parameters, other parameters (Glover-Rowe, crossover frequency ω_c, and R-value) were calculated to characterize overall brittleness and cracking susceptibility of tested binder, based on the master curve. These parameters and calculation methods are introduced later in this chapter.

2.1.3.2 Bending Beam Rheometer

The BBR test is used to characterize the low temperature performance of asphalt binder based on the PAV-aged binder residue. Two parameters are conducted during this test. One is flexural creep stiffness, which indicates the thermal stress, and the other is m-value, which indicates the ability to relax stresses and resist thermal cracking. AASHTO specifies the maximum measured stiffness as 300MPa and places the minimum m-value at 0.300. According to ASTM D6648 X1.5, stiffness and m-value are calculated as follows:

$$S(t) = P\,L^3/4\,bh^3\delta(t) \tag{2.3}$$

where $S(t)$=time-dependent flexural creep stiffness, MPa; P=constant load, N; L=span length, mm; b=width of beam, mm; h=depth of beam, mm; and $\delta(t)$=deflection of beam.

$$m - value = \left|\frac{d(logS(t))}{d(logt)}\right|_{t=60s} \tag{2.4}$$

Figure 2.8 BBR equipment used in this study

The basic BBR test uses a small asphalt beam (Figure 2.9) that is simply supported and immersed in a cold liquid bath. A load is applied to the center of the beam and its deflection is measured against time. Stiffness is calculated based on measured deflection and standard beam properties, and a measure of how the asphalt binder relaxes the load-induced stresses is also recorded. The test is run in accordance with ASTM-D6648.

Figure 2.9 BBR mold and sample preparation

2.2 Related Rheology Parameters

In this study, in addition to the rutting parameter and fatigue parameters from Superpave, some additional parameters (Glover-Rowe, crossover frequency, and R-value) were used to detect the brittleness of binder and to characterize the aging level of the same.

2.2.1 Glover-Rowe parameter (GR)

In addition to the rheology parameter from Superpave, the Glover-Rowe parameter (Rowe, 2014) can be used for predicting cracking performance. Glover consider a mechanical form for ductility test involving springs (G') and dashpots (η') to describe the behavior deduced that there was a relationship between cracking and $G'/(\frac{\eta'}{G'})$. The assumption was then proven by Anderson et al.; after Rowe's analysis, the GR parameter becomes $G * (\cos\delta)^2/\sin\delta$.

Because the frequency is constant, the GR parameter is a function of G and δ. At 15°C, the criteria of GR parameter is 180 kPa, in the limiting value of 9E-04 mPa/sec at 0.005 rads/s for the onset of cracking (very beginning of starting cracking). As for the second value suggested by Anderson et al., which presents the development of significant cracking, the criteria of GR parameter is 450 kPa. The limiting values are listed below, and for a better understanding can be plotted in the Black space diagram (Figure 2.10).

Damage onset: $$G * \frac{(\cos\delta)^2}{\sin\delta} = 180 \text{ kPa} \quad (2.5)$$

Significant cracking: $$G * \frac{(\cos\delta)^2}{\sin\delta} = 450 \text{ kPa} \quad (2.6)$$

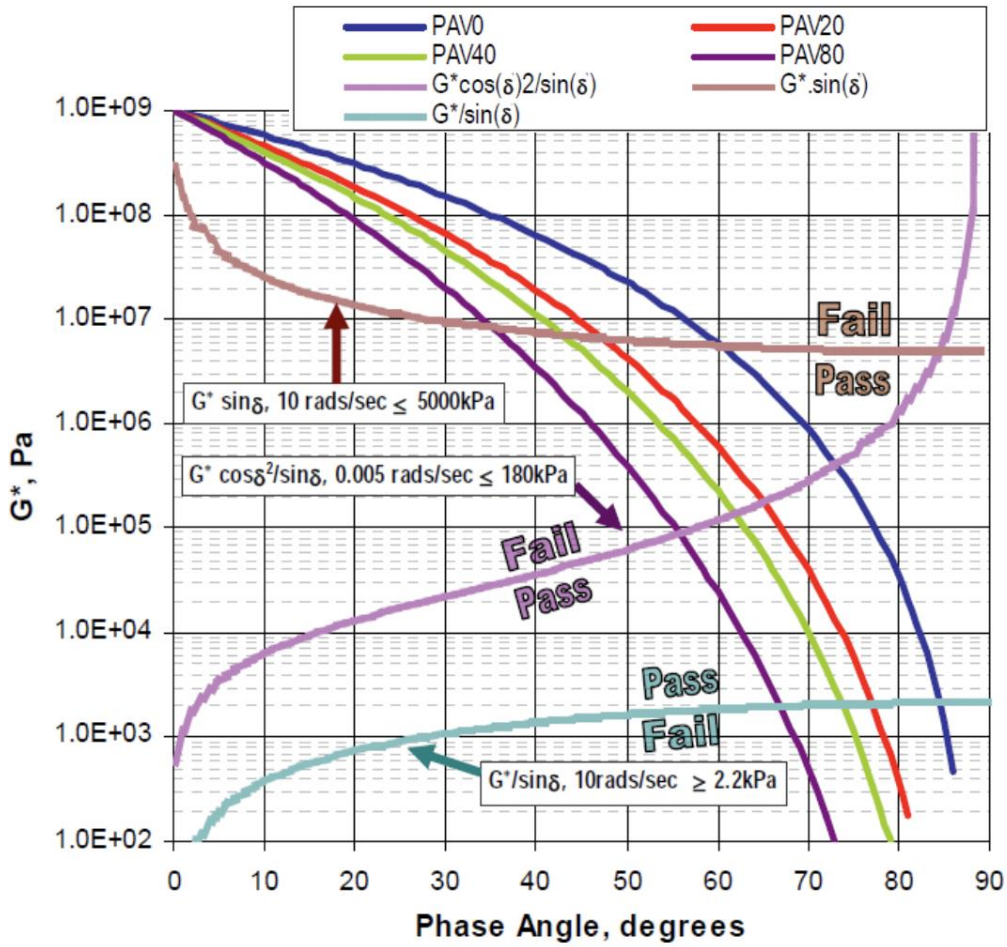

Figure 2.10 Criteria of GR parameter plot on a Black space diagram (Rowe, 2014)

2.2.2 Cross-over frequency (ω_c) and R-value

The crossover frequency is the reduced frequency where the loss and storage moduli are equal; that is, when the phase angle becomes 45 degrees. The R-value was also found to increase with asphalt aging. The R-value is defined as the difference between the log of the glassy modulus (which is 10^9 pa) and the log of the modulus at crossover frequency (Mogawer et al. 2016), for both R-value and crossover frequency, the reference temperature should be 15°C. The crossover frequency found decreasing with aging and R-value increasing with aging, as shown in Figure 2.11.

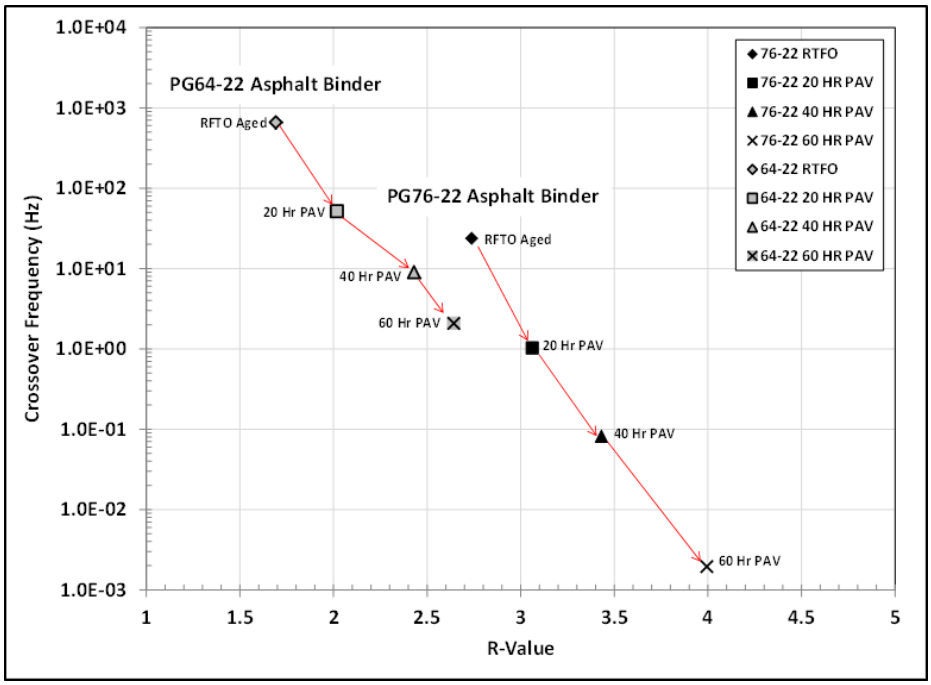

Figure 2.11 Crossover Frequency – R-value Space: PG64-22 and PG76-22 asphalt binders after different aging levels. (Mogawer et al. 2015)

2.2.3 Critical ΔT_c Parameter

A parameter to indicate the low temperature brittleness can be derived from the BBR tests results is the critical ΔT_c parameter. The ΔT_c parameter was shown to be a promising indicator of low-temperature cracking representing the loss of relaxation and recovery characteristics of an asphalt binder when the parameter decreases. It is defined as the difference between PG stiffness temperature (the temperature when stiffness equals 300 MPa) and PG m-value temperature (the temperature when m-value equals 0.300).

Rowe concluded that the ΔT_c and GR parameter essentially describing the same behavior (Rowe, 2014). It was shown that ΔT_c decreases with aging to indicate an increase in brittleness. There are no specified criteria for this parameter, simply an empirical threshold of -5°C used in this thesis. Because of excessive brittleness, testing could not be conducted for RAS, even at intermediate temperature; therefore, the ΔT_c parameter was not calculated for RAS. This was found to be consistent with results reported by Willis et al. (2016).

2.3 Related Recent Study Results

This section summarizes the results of recent studies investigating and how pavement performance is affected by the use of reclaimed asphalt pavement (RAP) and recycled asphalt shingles (RAS) at the binder level or mixture level. Generally, most studies conclude that using RAP or RAS can increase rutting resistance and that the low-temperature grade also increases and becomes more sensitive to thermal damage depending on the type and amount of RAP or RAS.

Most state highway agencies allow contractors to use less than 5% RAS in AC (Abbas et al. 2013). Most state transportation departments allow between 10% to 20% RAP for the surface courses and higher percentages are allowed for base and intermediate courses. Softer binder has also been suggested for use with AC with RAP to improve workability (Al-Qadi et al. 2009).

The purpose of the study by Al-Qadi et al. (2009) was to characterize the mixing efficiency of different percentages of RAP with virgin asphalt binder. The results indicated that assuming 100% working binder of mixing, design with RAP may be acceptable. Some performance tests showed that the amount of RAP increased the stiffness of AC. Brittle AC may lead to low-temperature cracking, and AC with RAP has the potential to reduce stripping, perhaps because of the strong binder–aggregate bonds of RAP. The study recommends that more extensive performance testing be implemented to investigate the rutting, fatigue, and low-temperature performance of AC mixes containing high percentages of RAP.

In Colbert et al. (2012) study, virgin binder was blended with 30%, 50%, 70%, and 100% RAP before evaluating the effects of aging, rolling thin-film oven (RTFO) aging, and pressure aging vessel (PAV) aging. The study found that the higher viscosity of binder blends with RAP and that further aging results in a continuous increase of stiffness.

Abbas et al. (2013) concluded that with additional RAS (0%, 5%, 7% and 10%), the asphalt binder becomes stiffer and harder to mix and to handle; as such, it was suggested that a softer base binder be used when RAS is added to AC. The results from this study showed an increase of G^* and a decrease of δ at high service temperature, which indicated a higher rutting resistance with additional RAS (Figures 2.12). While at intermediate temperature, there was no difference between $G^*\sin(\delta)$ with addition of RAS (Figure 2.13), which was inconsistent with

previous studies that reported a decrease fatigue resistance of AC mixtures containing RAS (Abbas et al. 2013). It was concluded that the fatigue parameter $G^*\sin(\delta)$ of Superpave may not be sufficient to characterize the fatigue behavior of asphalt binder at intermediate temperature.

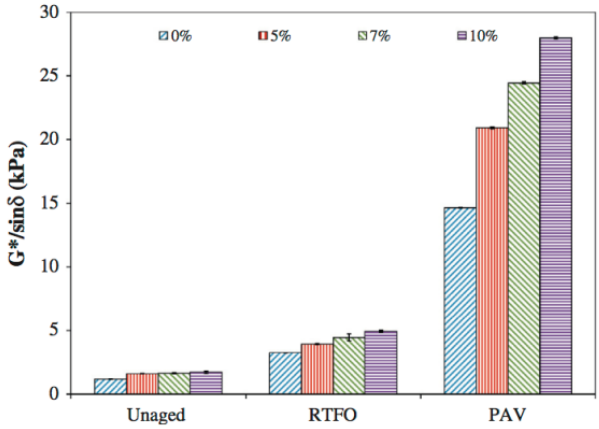

Figure 2.12 G*/sinδ at 58 ℃ and 10 rad/s (Abbas et al. 2013)

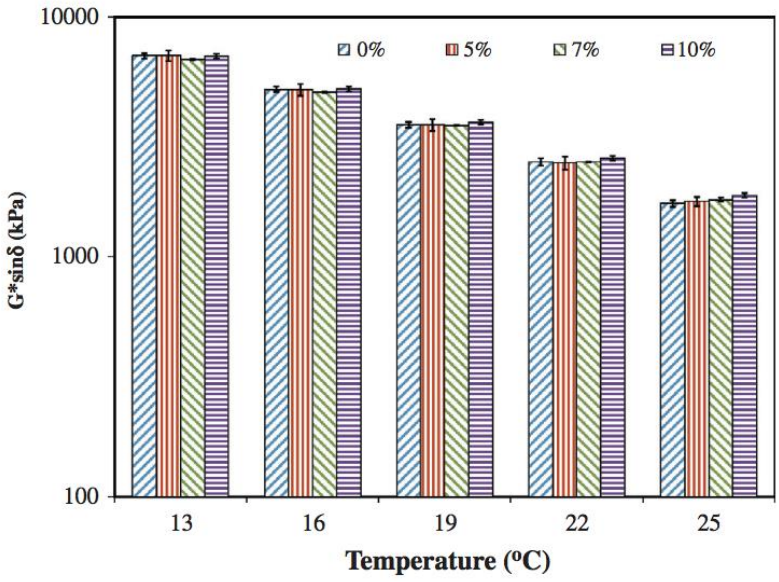

Figure 2.13 Fatigue parameter comparison for binder containing different RAS level (Abbas et al. 2013)

Huang et al. (2014) tested four binder sources and shifted them to a 20℃ reference temperature; the results are shown in Figure 2.14. Data were obtained at the region of frequency from 0.1 to 100 rad/s under the controlled 1% strain loading conditions with the temperatures of

-20, 0, 20, 40, 60 and 80℃. The two fresh binders—AAA-1 and AAC-1—showed similar rheology characteristics at either high or low temperature ranges. The AC with recent RAP from Manitoba was much stiffer than the two fresh binders, but softer than that with old RAP. The old RAP from South Carolina processed the highest complex modulus and the lowest phase angle, and these behaviors are typical features of highly oxidized-aged binders. Figure 2.15 shows the control binder blended with different percentages of RAP binder, with the master curve shifted to 13℃. The results clearly showed that the complex modulus increased with RAP content (Zhou et al. 2013).

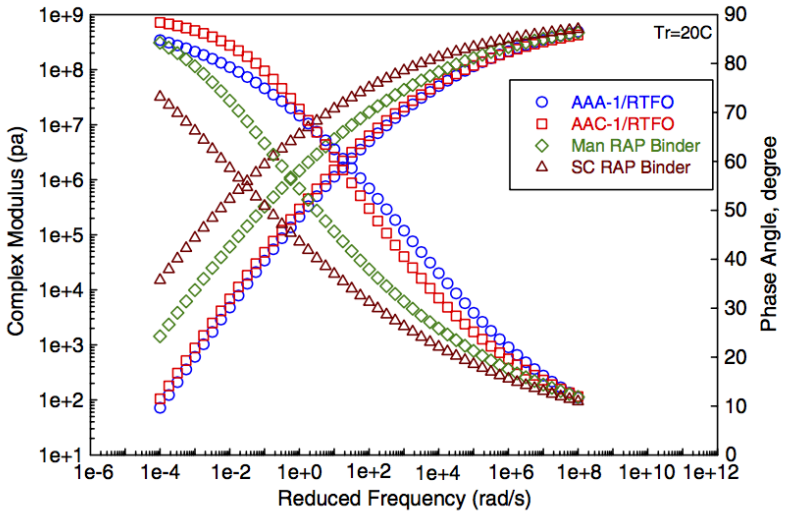

Figure 2.14 Complex modulus and phase angle for four materials (Huang et al. 2014) SHRP asphalt AAA-1 AAC-1; Man RAP (recent RAP); SC RAP (old RAP).

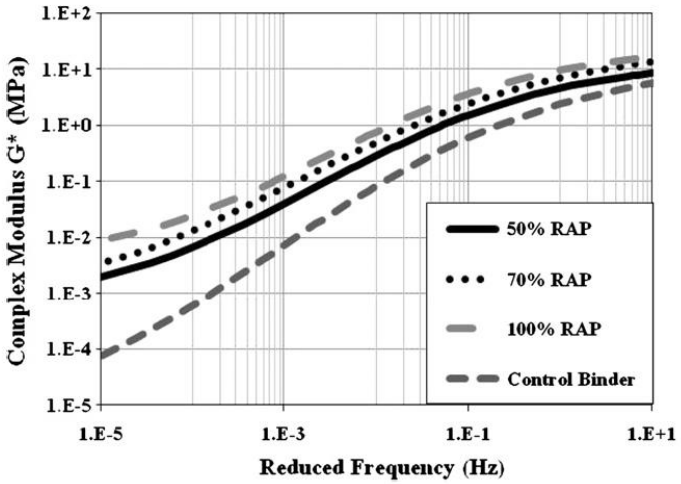

Figure 2.15 Master curve shift to 13°C for binder containing various RAP contents (Zhou et al. 2013)

Two parameters are obtained from the BBR test. One is flexural creep stiffness, which indicates the thermal stress; the other is m-value, which indicates the ability to relax stresses and resist thermal cracking (Abbas et al. 2013).

Results from BBR shown in Figure 2.16 indicates a clear increase of creep stiffness and a decrease of m-value with RAS content increasing. This suggests that additional RAS would result in increasing thermal cracking potential even if less than 10 percent (Abbas et al. 2013). Similar results are shown in Figure 2.17 with RAP content from 0 to 100%; the stiffness increased and m-value decreased when RAP's content increase (Khosla et al. 2012).

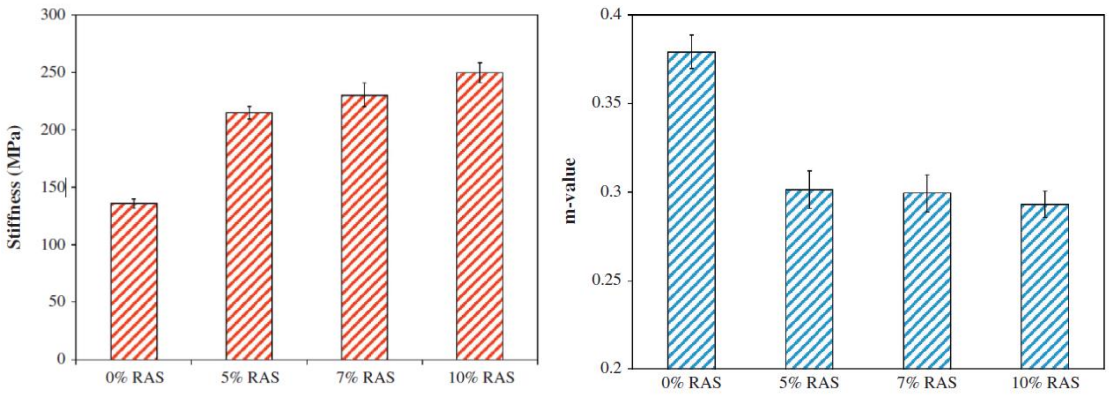

Figure 2.16 BBR test results for PAV-aged binders at -18 °C (Abbas et al. 2013)

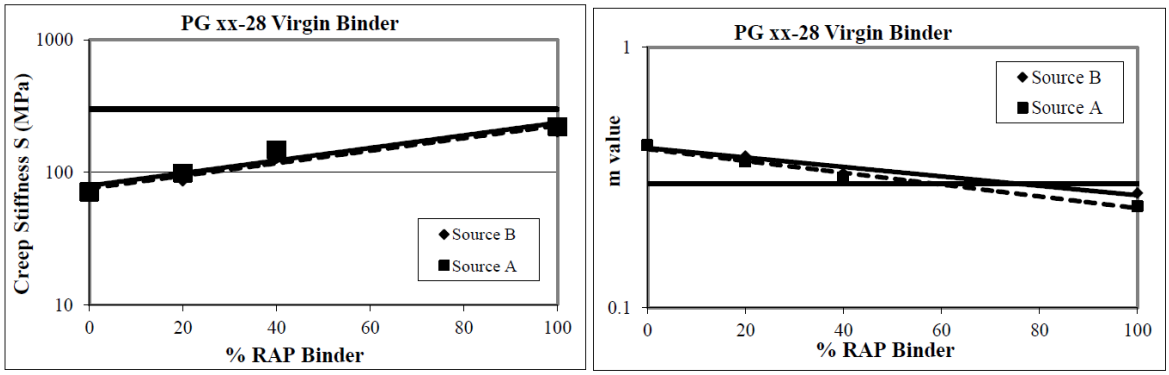

Figure 2.17 Creep stiffness and m-value versus RAP content (Khosla et al. 2012)

Figure 2.18 presents both high and low Superpave grades versus RAP content. It showed that blending binder grades varied affected by the base binder, and types of RAP and generally both the high and low temperature grade increased with RAP content. The same trends are showed in Figure 2.19, both the high-temperature and low-temperature grades increased with RAS content (Zhou et al. 2013).

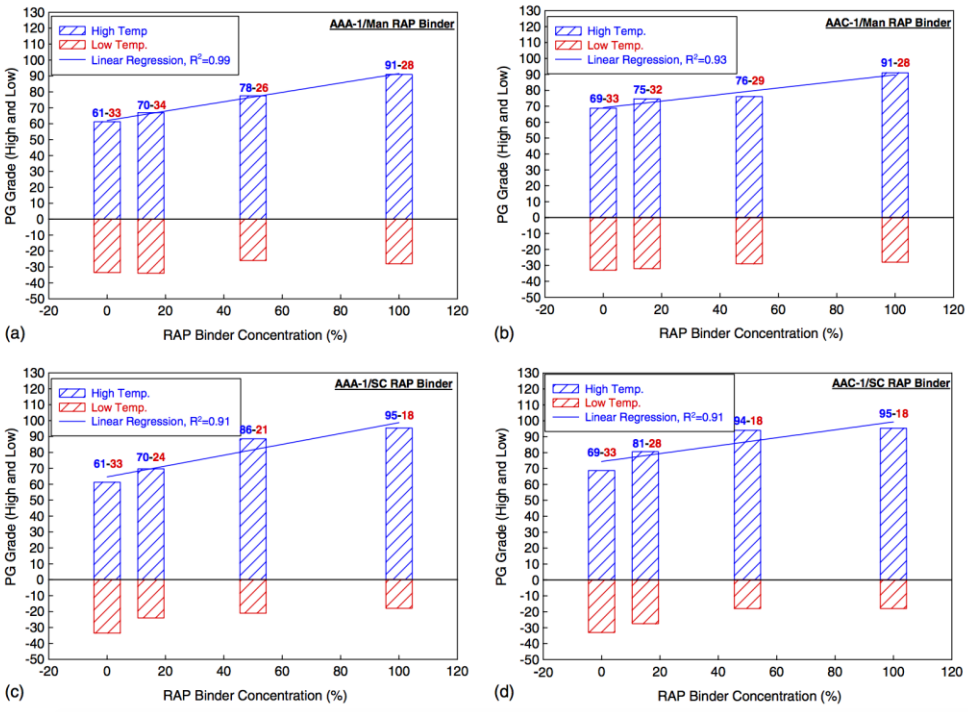

Figure 2.18 PG grading of different blending results (Huang et al. 2014) (SHRP asphalt AAA-1 AAC-1; Man RAP(recent RAP); SC RAP (old RAP))

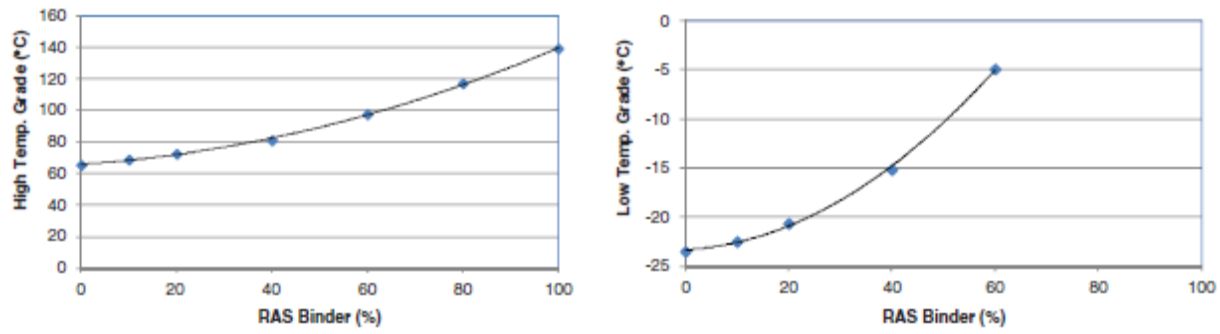

Figure 2.19 Binder blending grades (Zhou et al. 2013)

The GR parameter, plotted in Black space diagram (the y-axis is complex modulus and the x-axis is phase angle), is shown in Figure 2.20 (Mogawer et al. 2015). This study did not include use of recycled materials or the effects of ABR, but did examine the highly aged material properties in AC mixes. As shown in Figure 2.21, there were two types of binder (PG76-22 and PG 64-22) and four aging condition with each of them (RTFO, 20 PAV, 40 PAV and 60 PAV). The two red lines in the figure are the two criteria of GR (the dashed one is for onset cracking and the other one is for significant cracking), and as the aging condition increased the same trend can be observed for each material in which the complex modulus increased while the phase angle decreased and the points moved to the fail side.

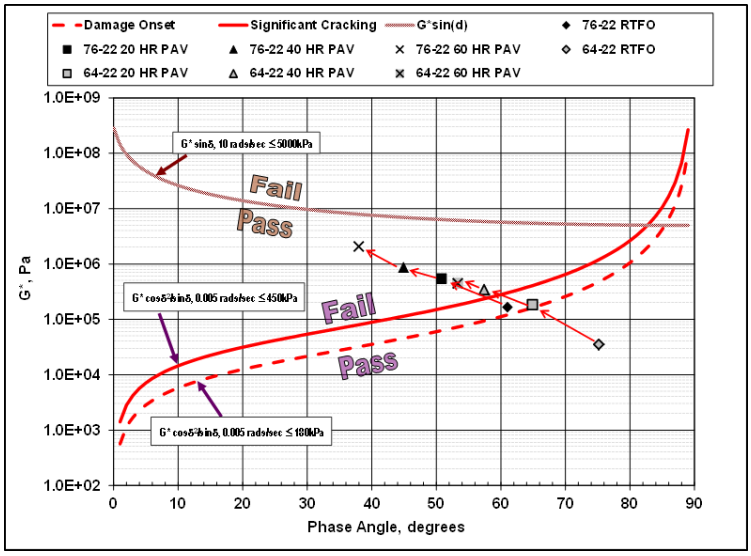

Figure 2.20 PAV-aged binders passing through the Glover-Rowe damage zone (Mogawer et al. 2015)

To summarize, the aforementioned studies emphasize the need for reliable AC and binder performance test methods and criteria to evaluate AC containing high recycled content or binders. Because the performance of blended binders and AC with recycled content after long-term aging has not been clearly understood, limits were generally determined based on engineering judgment or plant production capacity rather than using experimental characterization, supported with field results. Therefore, this study is aimed at investigating the rheology performance of a blend of RAS, RAP and virgin binders used in highway construction.

CHAPTER 3 TESTING METHODOLOGY AND MATERIALS

This chapter presents the detailed information about material using and testing implementation. All of the materials used in this study are from project ICT-R27-162: AC mixtures, virgin binders used in AC mixtures, RAP and RAS used in AC mixtures. Section 3.1 introduces the control binder type and RAS/RAP content of each AC mixtures. Section 3.2 presents the binder recovery from AC mixtures, aging history of virgin and extracted binder, and the details of DSR and BBR tests.

3.1 Materials

Three binder sources were used in the study: original binders were used in the preparation of AC (as the control binder); binders were recovered from recycled constituents (RAP and RAS) used in the AC; and binders were recovered from laboratory-designed and -produced mixes with ABR content of varying percentages (0%, 10%, 20%, 30%, and 60%). Table 3.1 presents a complete list of binder sources. The laboratory-prepared AC mixtures (N90) in accordance with Illinois Department Transportation specifications were designed in a previous study to develop the most effective mixture performance testing protocol to ensure cracking resistance (Al-Qadi et al. 2015; Ozer et al. 2016). These ACs were chosen for the current study because they were designed using stringent volumetric criteria, starting by changing the ABR level gradually, from a parent control AC design. In addition, complete AC mixture performance test results exist for these AC and can be used for correlation (Al-Qadi et al. 2015). Control binders used in the mixes were PG 52-34, PG 58-28, and PG 64-22. In this study, PG 58-28 and PG 64-22 were investigated and compared with the results from extracted binders. Because PG 52-34 is not commonly available or used in AC in Illinois or elsewhere in the United States, it was excluded from the testing program. Two RAP and RAS sources were included in this study to evaluate source variability.

Table 3.1 Binder Sources and AC Design Properties Used in the Experimental Program

1. Original Binders			
PG 58-28	PG 64-22		
2. Extracted Binder from Recycled Constituents (RAP and RAS)			
Binder ID	Source	Binder Content (%)	
RAP1	District 5	5.5	
RAP2	District 5	3.9	
RAS1	Source 1	26.7	
RAS2	Source 1	27.4	
3. Extracted Binders from AC			
Binder ID	Base binder of AC	RAP and RAS source of AC	ABR
N90-0[1] AS[2]	PG 64-22	0.0%	0.0%
N90-10	PG 64-22	2.5% RAS1	10.5%
N90-20	PG 58-28	5.0% RAS1	21.2%
N90-30	PG 58-28	7.0% RAS1	29.8%
N90-60 AS	PG 52-34	7% RAS2 + 20% RAP1 + 20% RAP2	60.8%

[1] N90-0, N90-10, N90-20, N90-30, and N90-60 indicate N-design and ABR percentage
[2] AS: 1% of Pavegrip 550 anti-strip was added to the total binder weight for some of the AC to reduce stripping potential and meet the tensile strength minimums and ratio requirements

3.2 Rheology Tests Implementation Details

3.2.1 Binder Recovery

The standard Rotovap test procedure mentioned in 2.1.1 was used to extract asphalt binder from the AC (N90-0 AS, N90-10, N90-20, N90-30 and N90-60 AS) and RAP/RAS (RAP1, RAP2, RAS1, and RAS2).

3.2.2 Aging history

ASTM D2872 Rolling Thin-Film Oven (RTFO) and ASTM D6521 Pressurized Aging Vessel (PAV) were used to simulate the short-term and long-term aging of virgin binders, respectively.

Aging protocols applied to the samples include standard (RTFO, PAV) and non-standard extra-long-term aging procedures (2PAV). The 2PAV means conducting another standard PAV aging on the PAV aged residues. The aging history for each sample is as follows:

- Control binders were subjected to RTFO, PAV, and second PAV (2PAV) protocols in addition to testing without any aging.
- Extracted binders from AC mixtures were tested as-is and after one PAV.
- Extracted binders from RAP and RAS were tested as-is.

3.2.3 Dynamic Shear Rheometer

The high-temperature grading was obtained from DSR in accordance with the Superpave specifications developed by the Strategic Highway Research Program (SHRP); $G^*/\sin\delta$, defined as the rutting parameter and the minimum limit was placed at 10 rad/sec (1.59 Hz): for un-aged binder it was 1.0 kPa, and for RTFO-aged and extracted binders it was 2.2 kPa. The high-temperature grading tests were conducted on un-aged, RTFO-aged and extracted un-aged binders at high temperature. For each test, two replicates were used to obtain the final results.

The temperature-frequency sweep tests were conducted on the virgin, RTFO-, PAV-, and 2PAV-aged control binders (PG 58-28 and PG 64-22), as well as on the un-aged extracted and PAV-aged extracted materials. All DSR data were obtained within the strain range from 0.05% to 5%, and the test was performed at a range of temperatures from 15°C to 64°C or 76°C (depending on material properties) at 12°C intervals. Test frequency was from 0.1 to 100 Hz at each temperature. Parallel plates of 8 mm diameter with a 2 mm gap were used at 15°C, 28°C, and at 40°C if the binder was too stiff; a 25 mm diameter plate with a 1 mm gap was used at temperatures greater than 28°C or greater than 40°C (depending on material properties). The master curves were constructed using MEPDG sigmoidal fit and shifted to a 28°C reference temperature. Two replicates were used to determine the final master curve of each material.

The outcome of the temperature-frequency tests are master curves defining the complex modulus G^* and phase angle δ across a wide range of temperatures and frequencies. Additional parameters (Glover-Rowe, crossover frequency ω_c, and R-value) were calculated to characterize overall brittleness and cracking susceptibility. The methods used to calculate these additional parameters as introduced before are as follows:

- The Glover-Rowe parameter is found using the expression $G * (\cos\delta)^2/\sin\delta$ measured at 15°C and 0.005 rad/sec. The criterion for onset damage is 180 kPa, and for significant cracking it is 450 kPa (Rowe 2014).
- The crossover frequency is defined as the frequency where the loss and storage moduli are equal to each other—that is, when the phase angle became 45 degrees.

- The R-value was found to increase with asphalt aging. It is defined as the difference between the log of the glassy modulus and the log of the modulus at crossover frequency (Mogawer et al. 2016).

3.2.4 Bending Beam Rheometer

The BBR tests were conducted on PAV and 2PAV aged control binders (PG58-28, PG64-22), un-aged, and PAV-aged extracted N90 binders. Stiffness, m-value, and ΔT_c were calculated for each tested binder.

In this study, four replicates were used for the tests of PAV-aged control binders and un-aged extracted binders. Because of limited material, only two replicates were tested for the 2PAV control binders and PAV-aged extracted binders.

CHAPTER 4 RESULTS AND ANALYSIS

This chapter presents the results obtained from various rheological tests for the binders aged in the laboratory and extracted from mixes.

4.1 Superpave Grading Results

Table 4.1 shows the Superpave grading results of all binders at various short- and long-term aging conditions. All the un-aged control binders were graded based on the Superpave specification that $G^*/\sin\delta > 1.0$ kPa. RTFO-aged and un-aged extracted binders were graded following $G^*/\sin\delta > 2.2$ kPa. The results from Table 4.1 show that all the virgin and RTFO-aged control binders met the Superpave specifications.

Table 4.1 Superpave Grading Results for Control and Extracted Binders

Binder Type	S(t) (MPa)	m —	$G^*/sin\delta$ @ un-aged (kPa)	$G^*/sin\delta$ @ RTFO (kPa)	$G^*sin\delta$ @ PAV (kPa)	Base Binder	Resultant Continuous Grade (CG)	Resultant Performance Grade
Original Binder								
PG 58-28	220	0.310	1.91	5.76	2155	—	CG 63.4-29.2	PG 58-28
PG 64-22	239	0.301	1.89	4.65	1737	—	CG 69.5-23.6	PG 64-22
Extracted Binder								
N90-0AS	219	0.302	—	2.39	3155	PG 64-22	CG 70.7-22.3	PG 70-22
N90-10	90	0.35	—	4.58	3168	PG 64-22	CG 69.7-21.0	PG 64-16
N90-20	78	0.326	—	2.70	1575	PG 58-28	CG 77.9-18.9	PG 76-16
N90-30	61	0.352	—	3.24	1259	PG 58-28	CG 79.3-16.0	PG 76-10
N90-60AS	53	0.303	—	2.27	880	PG 52-34	CG 88.2-10.7	PG 88-10
Extracted Constituents								
RAP1	107	0.349	—	2.84	1380	—	CG 90.1-14.0	PG 88-10
RAP2	159	0.316	—	2.66	1731	—	CG 77.6-24.4	PG 76-22
RAS1	—	—	—	256.77	—	—	CG 156.7-	—
RAS2	—	—	—	182.30	—	—	CG 150.1-	—

The high-temperature grades of RAS1 and RAS2 were above 150°C—much higher than those of other binders. The results showed that RAP1 was stiffer than RAP2 at high temperature, which was graded as 88°C; the average true grade of RAP1 was 90.1°C and RAP2 was 77.6°C. For the extracted N90 binders, generally the high-temperature grade increased with ABR content regardless of base binder grade. The true grades of N90-0AS and N90-10 with base binder of PG

64-22 were 70.7°C and 69.7°C, respectively. This finding indicated that after adding 2.5% RAS, the high-temperature grade changed very little. However, when the ABR content changed to 20% (N90-20), even with a softer binder of PG 58-28, the true grade increased to 77.9°C; for 30% ABR, it increased to 79.3°C. The N90-60AS, with the softest base binder of PG 52-34, has a true grade of 88.2°C.

The low-temperature grade shows that the PAV-aged PG 58-28 and PG 64-22 were graded as –28°C and –22°C, respectively, which met the Superpave specifications. The RAP1 was graded as –10°C and RAP2 as –22°C. For the extracted N90 binders (except N90-0AS), their low-temperature grade increased compared with that of their base binders. The N90-0AS with base binder of PG 64-22 was still graded as –22°C, but after its ABR content was increased to 10% (N90-10), it was graded as –16°C; the low-temperature grade increased by 6°C. For the N90-20 and the N90-30 with a base binder of PG 58-28, the low-temperature grade of the former increased by 12°C (to –16°C), and for the latter, by 18°C (to –10°C). PAV-aged N90-60AS was graded as –10°C with the softest base binder, PG 52-34; after approximately 60% recycled binder was added, its low-temperature grade increased by 24°C compared with the base binder. The results showed an increasing trend (warming) of low-temperature grade with ABR content regardless of base binder type, and the difference in low-temperature grades between the PAV-aged N90 series and their base binders increased as ABR content increased.

4.2 Complex Modulus Master Curves

This section presents the constructed master curves at 28°C reference temperature. Figure 4.1 is an overall plot of all evaluated ABR binders and Figure 4.2 shows the results for various combinations of extracted binders and control binders. The results are presented in each combination as follows:

- **Figure 4.2 (a)** presents original binders only at various aging conditions (un-aged, RTFO, PAV, and 2PAV) to evaluate aging impact on base binders used in the AC as well as extracted constituents. Binder modulus consistently increased with aging, as expected.
- **Figure 4.2 (b)** presents the results of RAP1 and RAP2 compared with 2PAV and PAV aged original binders. The RAP1 is stiffer than RAP2 and approaches the modulus values of the 2PAV aged PG 64-22.

- **Figure 4.2 (c)** presents recovered binders from low ABR mixes with their corresponding base binders (binders were recovered from N90-0AS and N90-10 with PG64-22 at all aging conditions). As shown in Figure 4.2 (c), there may be an equivalency of modulus between RFTO of virgin binder and extracted binder prior to PAV. When extracted binder was subjected to PAV, the same equivalency could be observed with the RTFO and PAV of corresponding base binder. None of the recovered binders before and after PAV could reach the values attained by 2PAV base binder.
- **Figure 4.2 (d)** presents recovered binders from high ABR mixes and with their corresponding base binders (binders were recovered from N90-20 and N90-30 with PG 58-28, N90-60AS with its RAP sources at all aging conditions). The equivalency noted in the previous curve no longer appears. RTFO and RTFO + PAV of base binder fell short of the extracted binder prior to PAV. The modulus curve of extracted binder is somewhere between the first and second PAV of base binders. When extracted binder was subjected to PAV aging, the modulus of N90-20 and 30 reached the stiffness of that of 2PAV PG58-28.
- **Figure 4.2 (e)** presents N90-60AS with its RAP sources (RAP1 and RAP2) and the 2PAV binders (PG58-28 and PG64-22). Because of adding 7% RAS2 even if with the softest base binder PG 52-34, before aging the modulus performed between the RAP sources while after PAV it was higher than its RAP sources. These results indicate that the binder present in high ABR AC is already at a severely aged state right after production.
- **Figure 4.2 (f)** presents recovered binders from AC with five different ABR levels (immediately after recovery and after PAV) to evaluate ABR levels in the AC. Binders recovered from AC with 60% ABR mixes (N90-60AS) had a significantly higher modulus than the others, even though this AC had the softest base binder (PG 52-34). One PAV shifted up the modulus curves by almost the same amount for all binders. It was also noted that there may be an equivalency between binders obtained from higher ABR mixes (such as N90-20 and N90-30) and the PAV of binders recovered from zero or low ABR mixes (N90-0AS and N90-10).

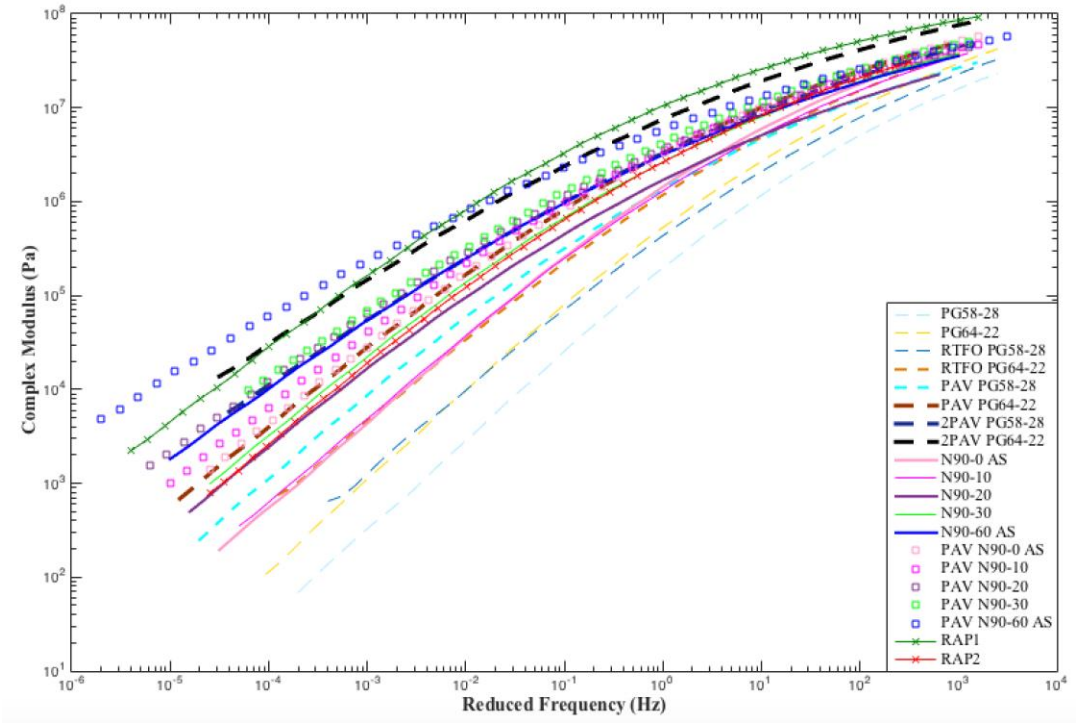

Figure 4.1 Complex modulus master curves for all studied ABR binders

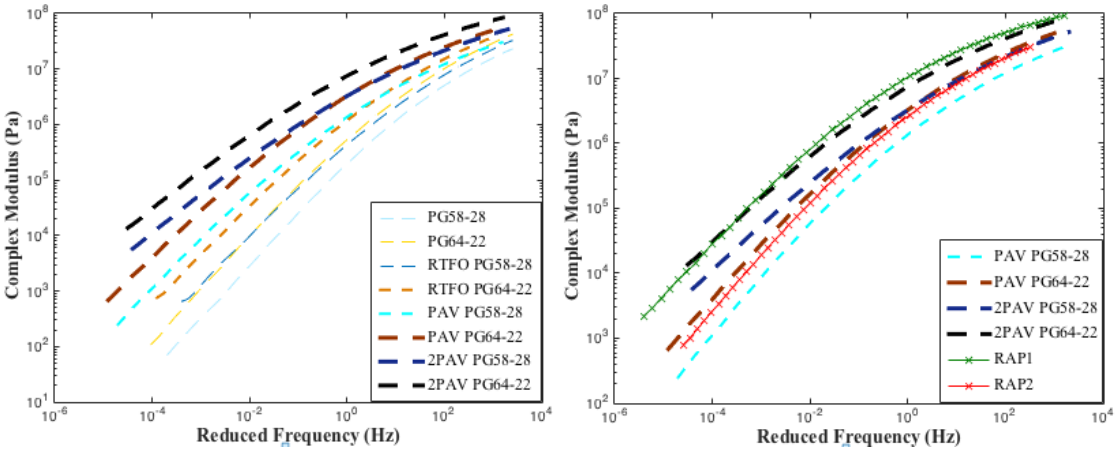

(a) (b)

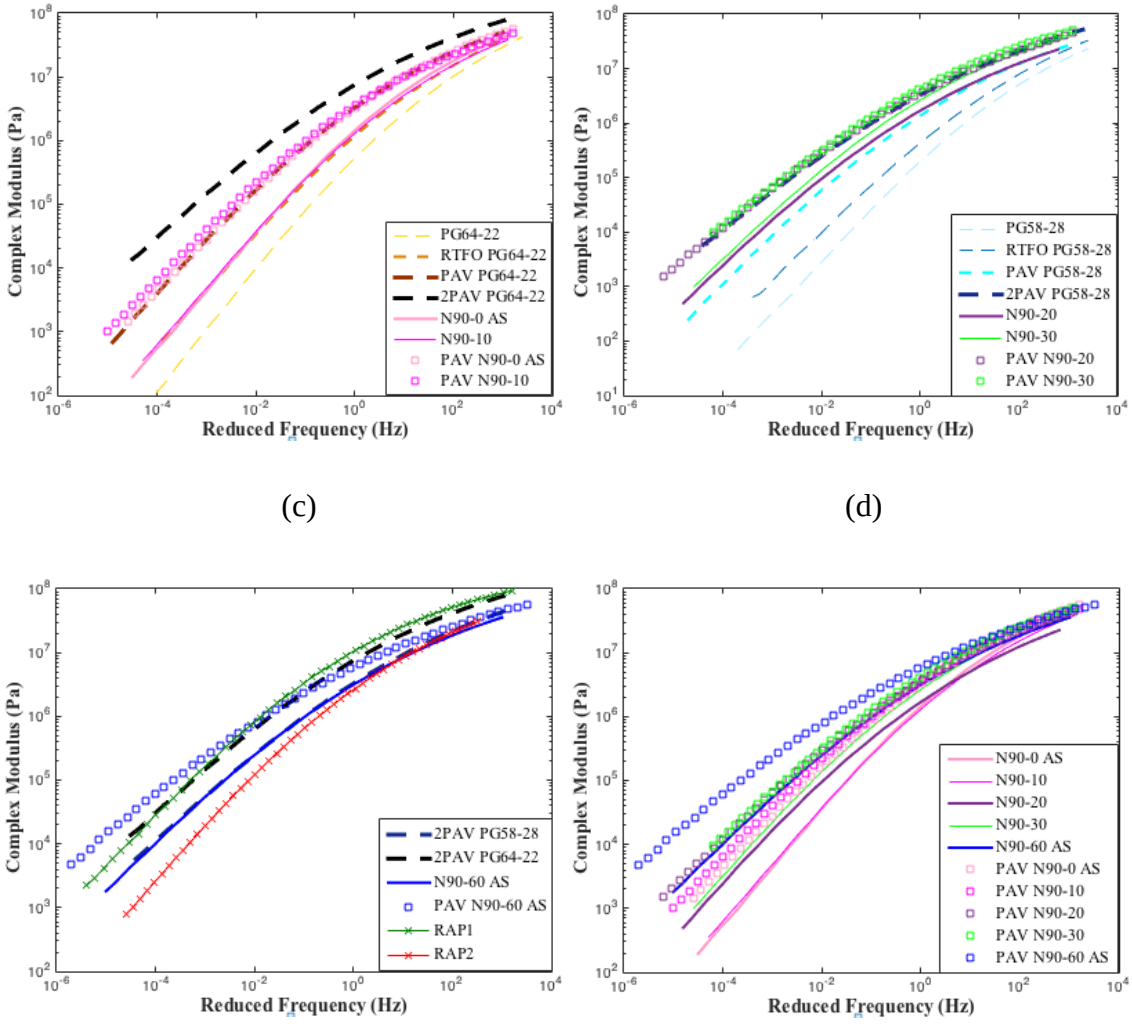

Figure 4.2 Subplot of complex modulus at reference temperature of 28°C (a) un-aged, RTFO-, PAV-, and 2PAV-aged control binders; (b) RAP with 2PAV- and PAV-aged control binders; (c) N90-0AS and N90-10 binders of two aging conditions compared with their base binder, PG 64-22, under four aging conditions; (d) N90-20 and N90-30 binders of two aging conditions compared with their base binder, PG 58-28, under four aging conditions; (e) N90-60AS with two aging conditions compared with its RAP source and 2PAV-aged control binders; (f) PAV-aged and un-aged extracted binders from AC.

4.3 Derived Rheological Parameters

To obtain a better understanding of ABR levels and aging on a binder's brittleness, additional parameters were used, as previously discussed. These parameters were ΔT_c obtained from low-temperature BBR, the Glover-Rowe parameter, R-value, and crossover frequency from

the DSR complex modulus tests. A summary of the additional rheological parameters is presented in Table 4.2. Each of these parameters is discussed separately.

Table 4.2 Results of Rutting, Glover-Rowe Parameter, Crossover Frequency, R-value, and ΔT_c

Virgin binder	Aging status	Rutting (kPa) 50°C; 10 rad/s	Glover-Rowe (kPa) 15°C; 0.005 rad/s	wc (Hz) 15°C	R-value 15°C	ΔT_c
PG 58-28	—	6.34	0.07	12,728	0.593	—
PG 58-28	RTFO	22.83	0.92	9,392	0.854	—
PG 58-28	PAV	79.09	23.65	312	1.733	0.39
PG 58-28	2PAV	231.59	207.69	28	1.866	–7.73
PG 64-22	—	13.35	0.66	11,488	0.466	—
PG 64-22	RTFO	41.22	6.77	2,403	1.210	—
PG 64-22	PAV	183.41	106.90	123	1.576	–0.26
PG 64-22	2PAV	536.55	757.65	8	1.740	–5.97
Extracted Binder						
RAP1		693.40	875.53	16	1.525	–5.37
RAP2		124.46	73.98	218	1.568	–2.44

ABR binder	Base binder	ABR content	Rutting (kPa)	GR (kPa)	wc (Hz)	R-value	ΔT_c
N90-0 AS	PG 64-22	0.0%	49.97	8.67	1,168	1.363	2.22
N90-10	PG 64-22	10.5%	44.67	10.10	899	1.464	1.45
N90-20	PG 58-28	21.2%	93.38	93.49	323	1.736	–4.12
N90-30	PG 58-28	29.8%	167.27	90.20	168	1.643	0.35
N90-60 AS	PG 52-34	60.8%	266.75	284.05	17	1.995	–8.69
N90-0AS PAV	PG 64-22	0.0%	158.47	116.03	192	1.507	–1.27
N90-10 PAV	PG 64-22	10.5%	227.15	187.12	78	1.680	–3.41
N90-20 PAV	PG 58-28	21.2%	378.24	243.69	14	1.964	–17.71
N90-30 PAV	PG 58-28	29.8%	342.12	280.88	21	1.823	–8.37
N90-60AS PAV	PG 52-34	60.8%	736.60	1269.90	1	2.336	–21.60

4.3.1 Rutting Parameter

The rutting parameter was derived using $G^*sin\delta$ at 50 °C and a frequency of 10 rad/s for each binder and its corresponding aging condition. Results are shown in Figure 4.3. A Higher value of rutting parameter indicates a higher resistance to rutting. The results showed that rutting parameter increased with aging as well as ABR content. The rutting resistances observed for unaged N90-0AS and N90-10, RTFO-aged PG 64-22, and PAV-aged N90-0AS were still close to those of the PAV-aged PG 64-22, while the rutting resistance for PAV-aged N90-10 was higher than for PAV-aged PG 64-22 and PAV-aged N90-0AS. When ABR contents increased to 20 and 30, compared with their base binder PG 58-28, rutting resistance increased significantly for unaged or PAV-aged status. The rutting parameter of unaged N90-60AS was higher than that

of PAV-aged PG 64-22, even though the base binder was PG 52-34 in this mix. After PAV aging, the rutting resistance of N90-60AS became nearly as high as that of RAP1.

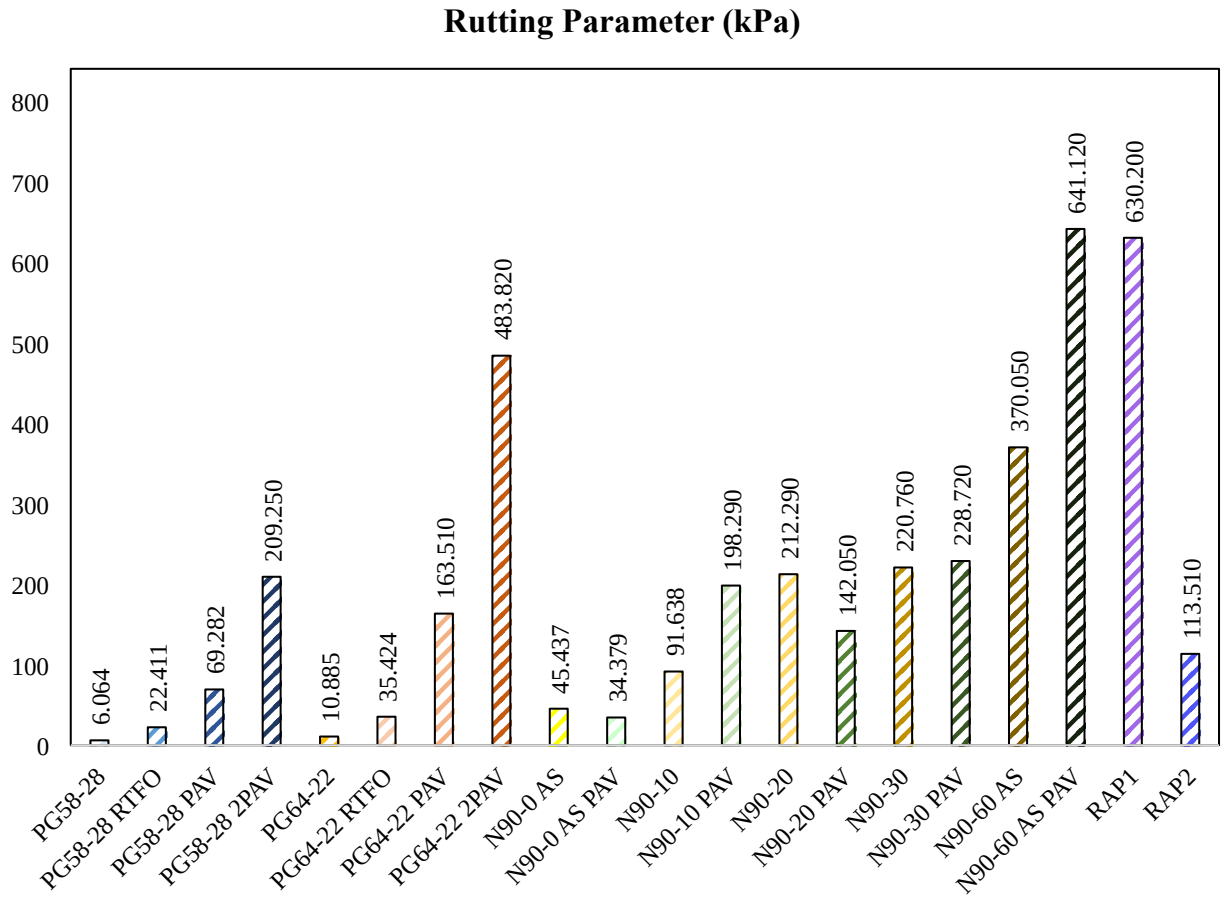

Figure 4.3 Bar chart of rutting parameter for all ABR binders

4.3.2 ΔT_c Parameter

As shown in Table 4.2, PG 58-28 and PG 64-22 had a relatively small ΔT_c , warmer than –1°C under PAV conditions. After 2PAV aging, the absolute value of ΔT_c for each binder decreased dramatically, to –7.73°C and –5.97 °C for PG 58-28 and PG 64-22, respectively. Other constituents used in the AC design of the N90 series—RAP1 and RAP2—had ΔT_c values around –5°C. Because of excessive brittleness, testing could not be conducted for RAS binder, even at intermediate temperature; therefore, the ΔT_c parameter was not calculated for RAS binder.

A consistent trend was observed with the ΔT_c for all extracted binders with increasing ABR and PAV. In general, the ΔT_c parameters were greater than –5°C, except for the binder with 60% ABR (N90-60AS), which had a value of –8.69°C. After PAV aging, a dramatic decrease was consistently observed for all the extracted binders—some had ABR values (30% and 60%) as high as approximately –20°C. Considering the empirical preliminary threshold of –5°C proposed for low-temperature susceptibility of binders, the AC with 60% ABR could experience brittleness in both the short and long terms.

4.3.3 Glover-Rowe Parameter

Figure 4.4 presents the Glover-Rowe parameter values in the black space diagram presented by complex modulus and phase angle. The solid lines represent onset damage, and the dashed line indicates the point at which significant fatigue damage happens. In general, these results present an expected behavior of binders moving from the lower right quadrant (high phase angle and lower modulus) to the upper right quadrant (lower phase angles and higher modulus indicating a decrease in viscous component). Figure 4.4 (a) is the plot of two control binders under all aging conditions. As aging increased, the values moved to the upper right quadrant, approaching the potential failure zones. The 2PAV PG 64-22 passed the significant damage line. As shown in Figures 4.4 (b) and (c), before PAV aging only the N90-60AS passed the onset damage. On the other hand, all binders except the N90-0AS passed the onset damage line or significant failure zone after PAV.

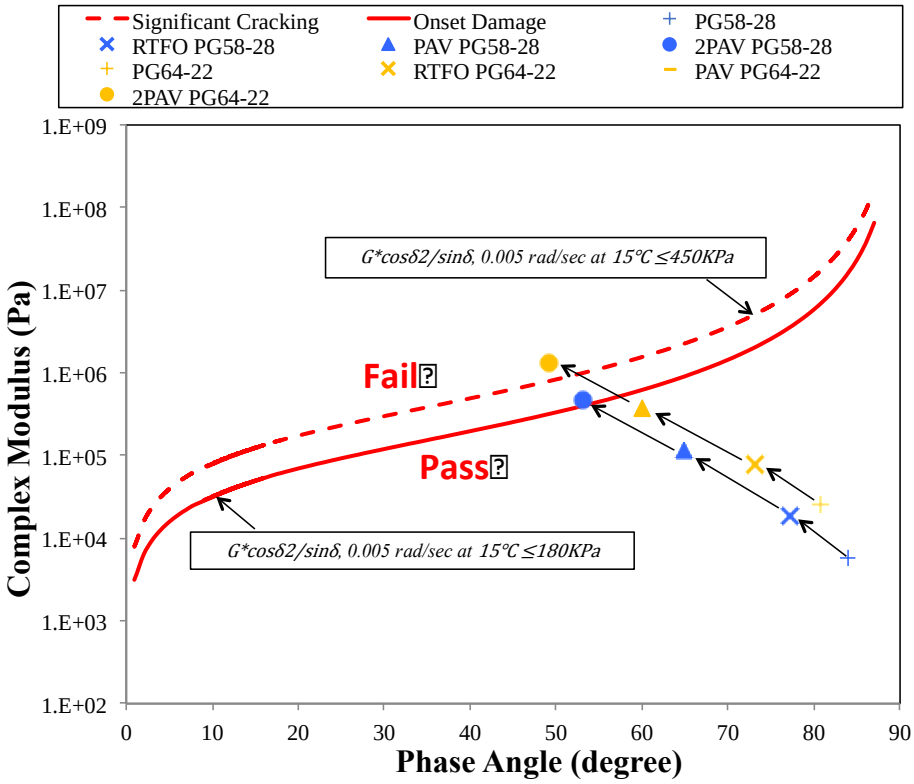

(a)

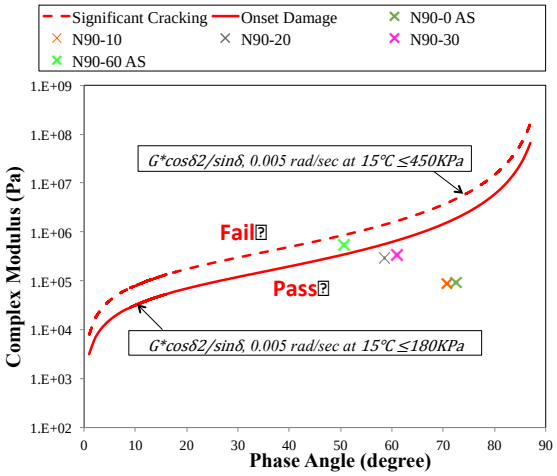

(b)

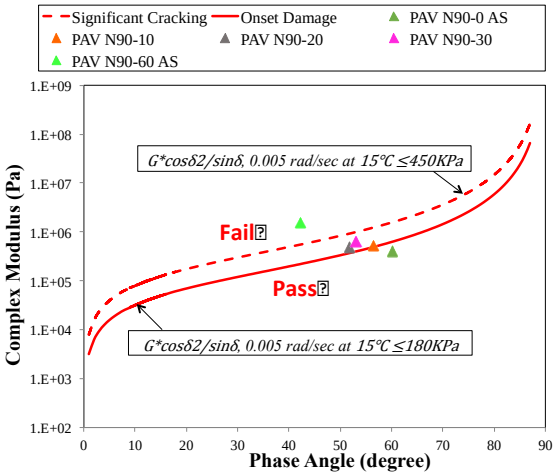

(c)

Figure 4.4 (cont.)

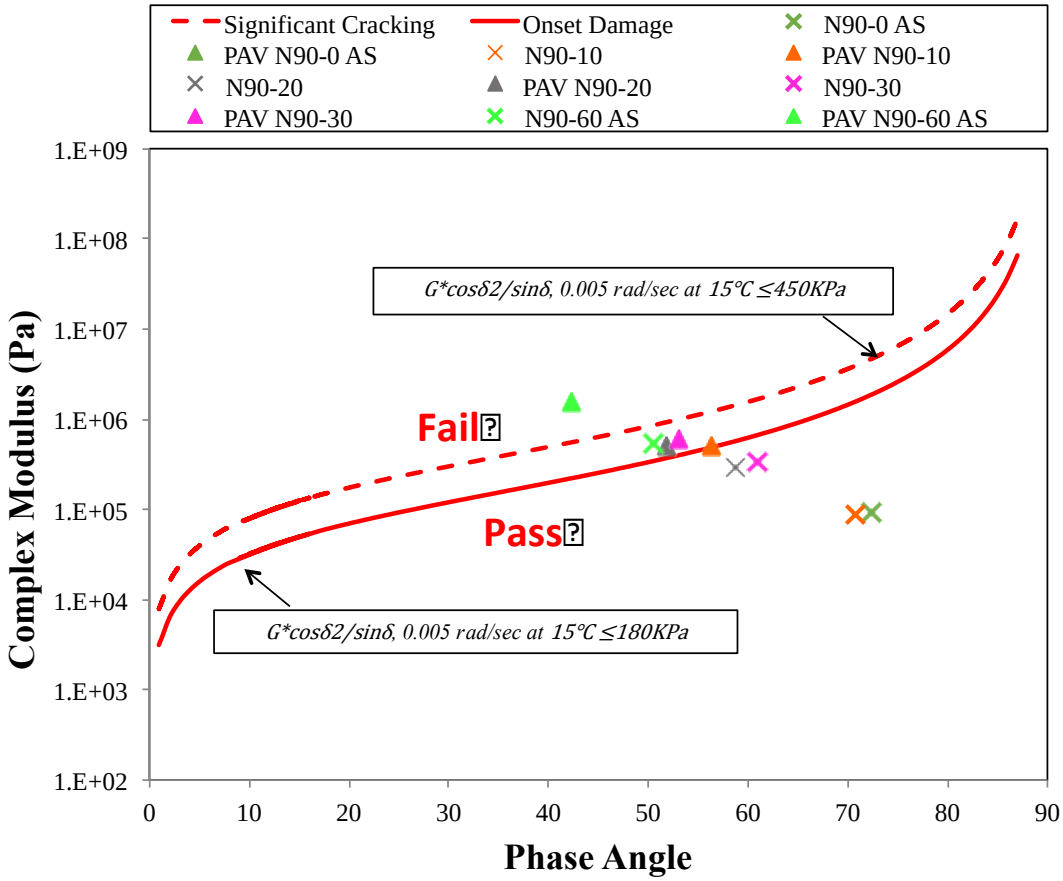

(d)

Figure 4.4 (a) Black space diagram of all aging conditions of PG 64-22 and PG 58-28 at 15°C and 0.005 rad/sec; (b) Black space diagram of un-aged extracted N90 series at 15°C and 0.005 rad/sec; (c) Black space diagram of PAV-aged extracted N90 series at 15°C and 0.005 rad/sec; (d) Combined picture (b) and (c)

4.3.4 R-value and Crossover Frequency

Figure 4.5 presents the plots of the crossover frequency and R-value results obtained by shifting the master curves to a reference temperature of 15°C. The crossover frequency is a measure of overall binder hardness, which should generally decrease with binder aging and is usually higher for oxidized binder (Rowe 2014; Ozer et al. 2016). Figure 4.5 (a) shows the results of control binders under all aging conditions as well as for the RAP. Consistent with previous studies, the crossover frequency decreased, and the R-value increased, with aging. The

R-value versus crossover frequency for the N90 series is shown in Figure 4.5 (b), generally as the ABR content increase the crossover frequency decreased and R-value increased at each aging condition.

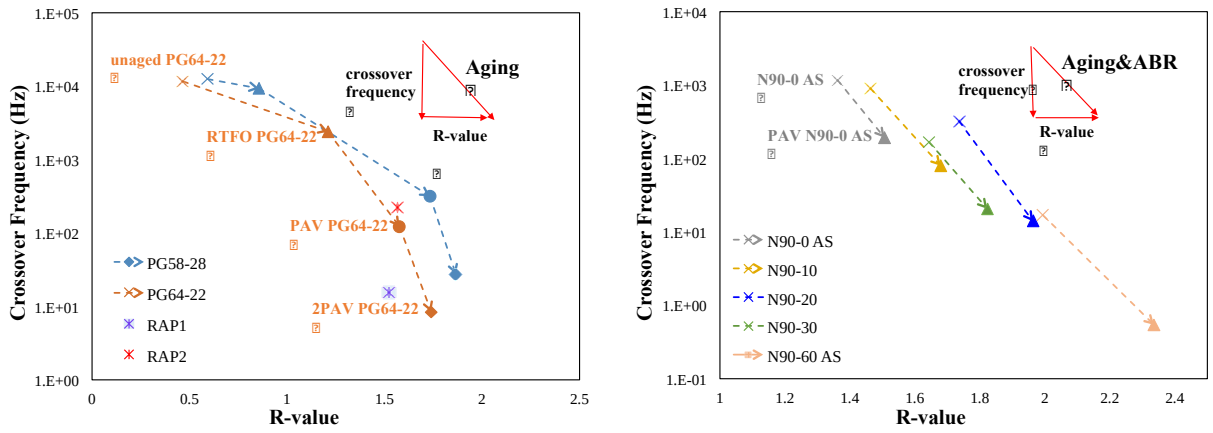

(a) (b)

Figure 4.5 (a) Crossover frequency versus R-value of control binders and RAP at a reference temperature of 15°C; (b) Crossover frequency versus R-value of extracted binders at a reference temperature of 15°C.

4.4 Equivalency of Aging and ABR Levels for Brittleness of Binders

There was a consistent trend with an increase in the ABR level; that trend can be helpful in evaluating brittleness of binders that would otherwise be masked within the Superpave grade changes. This section presents an evaluation of the additional rheological parameters used to determine critical ABR levels in AC.

Figure 4.6 illustrates the change in the ΔT_c parameter with aging of the original binders [Figure 4.6 (a)] and ABR level of extracted binders [Figure 4.6 (b)]. It is clear from the original binder data that the critical threshold of –5°C is exceeded only with the second PAV. An equivalency [not shown in Figure 4.6 (b)] could be established between extracted binder as-is and one PAV-aged base binders for the ΔT_c parameter only for low ABR content mixes. However, the ΔT_c parameter for extracted binders progresses much more rapidly when the ABR level increases to 20% and higher. Even before PAV was applied, AC with higher ABR levels (more than 20%, with the exception of 30% ABR) had ΔT_c values around critical thresholds.

After one PAV application, binders recovered from the high ABR mixes (20%, 30%, and 60% ABR) exhibited values well beyond the critical threshold of –5°C and beyond 2PAV corresponding binders (PG58-28 and PG52-34). It is important to note that the low and medium ABR mixes were prepared with RAS only (i.e., no RAP). The situation may not be as critical for AC with ABR 20% or 30% with RAP only or RAP and RAS because RAP binder exhibited moderate values of brittleness. It was also noted that when ABR levels are high, the PAV-aged extracted binder can have much more critical values of ΔT_c than the second PAV of their corresponding base binders.

Two performance issues can be inferred from this equivalency analysis. The first is that the binder in high ABR AC can be relatively more brittle immediately after production than their counterparts with no or low ABR. This finding indicates that these AC can have some short-term low-temperature cracking performance issues. A second and more important observation is the performance of these AC after aging. Laboratory environment PAV of extracted binders for high ABR AC indicates that these AC will age much faster than the binder in the AC with no or low ABR. Accordingly, it was concluded that the critical ABR level for AC with only RAS should be below 20%, which corresponds to below 5% RAS.

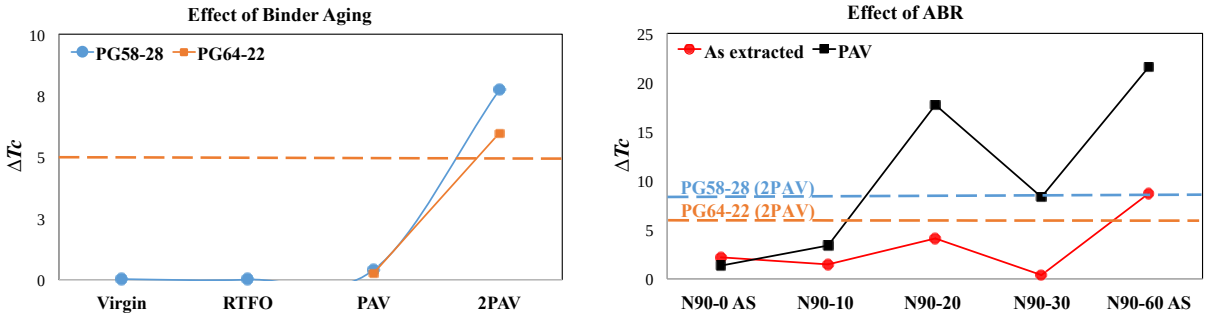

(a) (b)

Figure 4.6 (a) Comparison of the ΔT_c parameter with changing aging levels of control binders; (b) Comparison of the ΔT_c parameter with changing ABR and aging levels of extracted N90 binders

A similar analysis was conducted for the Glover-Rowe parameter as an indication of block and fatigue cracking. Figures 4.7 (c) and (d) show the results for the parameter with aging of original binders as well as the ABR levels for extracted binders. A clear and similar trend of an increase in the Glover-Rowe parameter with aging and ABR level was observed. Both base

binders reached the critical threshold proposed for cracking (180 kPa) after second PAV. For the extracted binders, the Glover-Rowe parameter consistently increased with increasing ABR and at a higher rate of increase at high ABR levels. The critical threshold of 180 kPa was reached for the binder with 10% ABR after PAV. As ABR increased to 60%, even before PAV, extracted binder exceeded the critical threshold.

Similar to the ΔT_c comparision for low ABR mixes, the Glover-Rowe values of extracted binder from low ABR mixes are equivalent to one PAV of their corresponding base binder; after PAV aging, it increased slightly compared with 2PAV of their base binder. When ABR levels are greater than or equal to 20%, a single PAV of the extracted binders exhibited much higher values of the Glover-Rowe parameter as the second PAV of their corresponding base binders. The gap between the parameters calculated between PAV of extracted and a 2PAV of the base binder increases at the highest ABR level. According to the progression in the Glover-Rowe parameters, the AC with high ABR content could negatively be impacted by short- and long-term brittleness that affects block cracking or fatigue cracking development. In addition, they could age much faster than their counterpart AC with low or no ABR—reaching a state of severe brittleness.

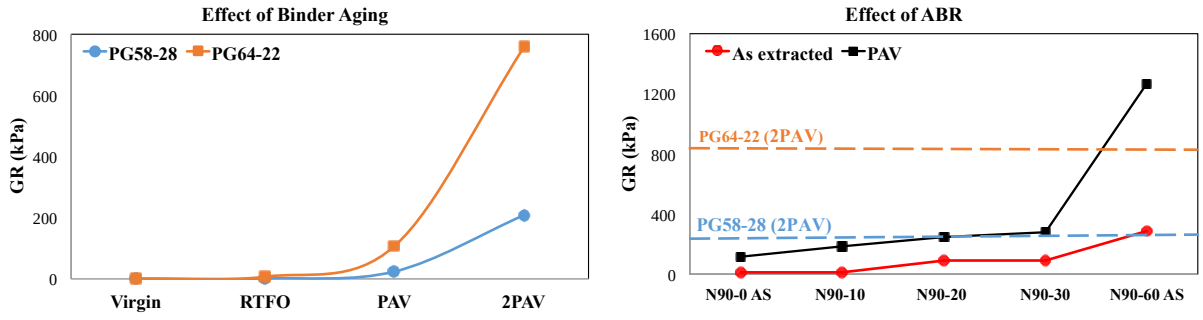

(a) (b)

Figure 4.7 (a) Comparison of the Glover-Rowe parameter with changing aging levels of control binders; (b) Comparison of the Glover-Rowe parameter with changing ABR and aging levels.

4.5 Correlation to Mixture Performance

Flexibility Index (FI) was developed as a parameter to characterize cracking potential of AC mixture, and it showed good correlation with field performance (Al-Qadi et al. 2015).

Generally good performance AC mixtures had FI values greater than 8.0, while more brittle mixes showed values lower than 4.0 (Al-Qadi et al. 2015). Figure 4.8 presents the plots of FI versus the GR parameter and ΔT_c of PAV aged N90 binders. As shown in Figure 4.8 (a) and (b), which represents the correlation between FI and as extracted N90 binders, generally the GR value and ΔT_c increased with FI decreased, which indicated these two parameters provided the similar failure trends as FI did. The same trend can be found from the results of PAV aged extracted N90 binders (Figure 4.8 (c) and (d)).

The FI showed when ABR content increased to 30%, the AC mixture exhibited poor performance, and the mix with 60% ABR showed a potential of extreme lack of flexibility to release stress. Before PAV aging, except N90-60 AS, the GR parameter of the extracted N90 binders are generally below 100 kPa and ΔT_c are below 5.0, which means these binders still possess good properties to relax stress and resistance cracking at intermediate or low temperatures, and the FI of the corresponding AC mixtures are higher than 4. After PAV aging, the GR parameter showed that when ABR reached 10% it was already exposed to onset failure, and the 20 and 30% ABR was in the range between onset damage and significant cracking. A similar trend was obtained from the relationship between the ΔT_c and FI, except N90-0 AS and N90-10; other binders' ΔT_c are much higher than 5, which means they are brittle at low temperatures.

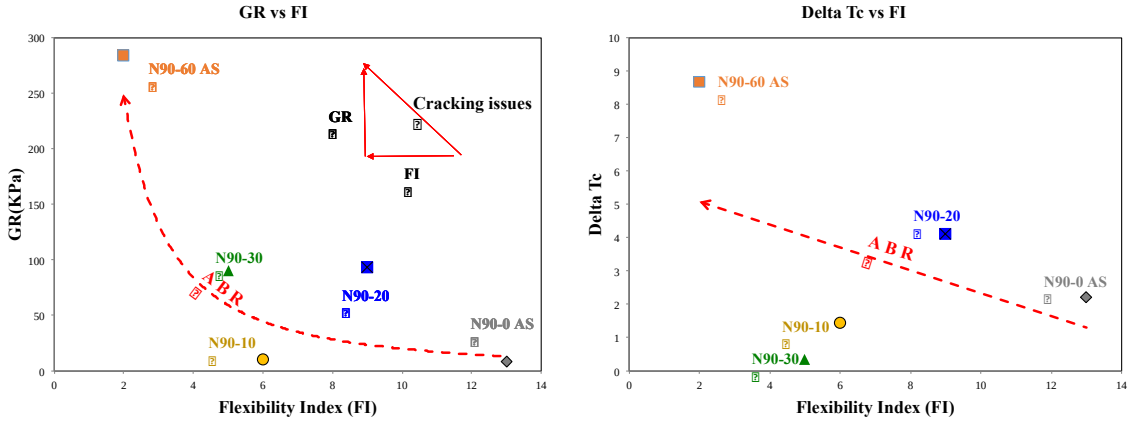

(a) (b)

Figure 4.8 (cont.)

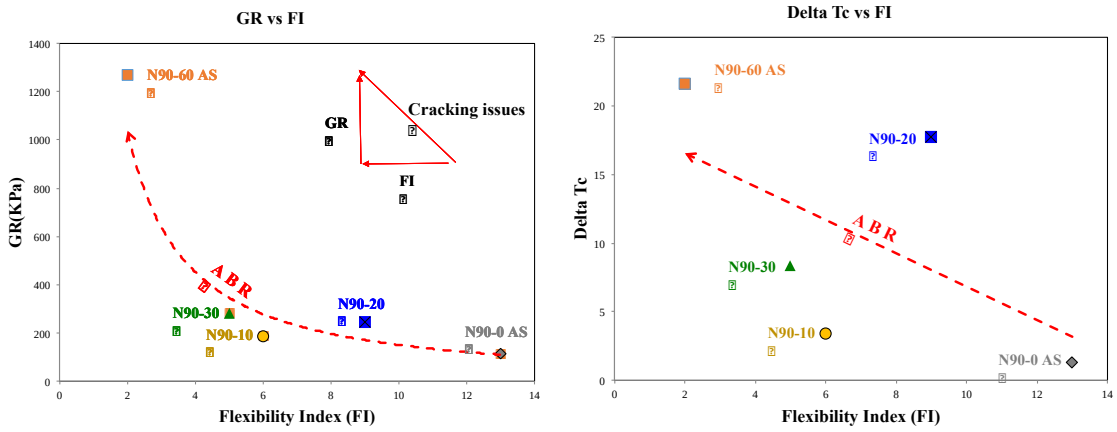

(c) (d)

Figure 4.8 (a) Correlation between Glover-Rowe of as extracted N90 binder and Flexibility Index; (b) Correlation between ΔT_c of as extracted N90 and Flexibility Index; (c) Correlation between Glover-Rowe of PAV aged N90 binder and Flexibility Index; (d) Correlation between ΔT_c of PAV aged N90 binder and Flexibility Index

CHAPTER 5 CONCLUSIONS AND RECOMMENDATIONS

This thesis presented an experimental evaluation of the rheological properties of binders from various sources: base binders used in design of asphalt mixes; recovered binders from the laboratory compacted AC with increasing ABR; and recovered constituents in the AC (RAP and RAS). The experimental program included the determination of standard Superpave grading and additional rheological parameters derived from various BBR and DSR tests: ΔT_c (for low-temperature cracking susceptibility), Glover-Rowe parameter, R-value, and crossover frequency (these last three parameters indicate block and fatigue cracking performance). Brittleness of binder was assessed using these parameters which would otherwise be masked within the changes in Superpave grade, unless the changes were highly significant. Based on the experimental results and calculated parameters, the following conclusions can be drawn:

- As the ABR level increased, both the high and low-temperature grades increased. Both high and low temperature grades of the extracted binder generally increased by one or two grades higher than its corresponding binder when ABR content was below 30%. In the case of the highest ABR level (60%), the high-temperature grade increased by six grades (from 52 to 88) and the low-temperature grade increased by four (from -34 to -10).
- Complex modulus values across a wide range of temperatures and frequencies clearly increased with higher aging level and ABR content, regardless of the base binder properties.
- The ΔT_c parameter increased with additional aging and increasing ABR levels. The proposed threshold of –5°C was exceeded by a wide margin when PAV was applied to the extracted binder recovered from AC with above 20% ABR. The values were in the range of –8°C to –21°C.
- Similarly, the effects of aging and ABR levels were observed in the Glover-Rowe parameters, especially after the additional PAV. All the base binders reached the critical threshold of 180 kPa only after the second PAV. The extracted binder from AC with 60% ABR had values exceeding the critical thresholds even before aging. The effect of ABR with RAP could be expected to differ from that of the AC with RAS only—resulting in more moderate changes in the progression of brittleness for AC with RAP only.

- The crossover frequency decreased and the R-value increased with aging level and increasing ABR for all the studied binders. However, there is more work needed to reliably calculate R-value with the modulus values recorded at lower temperatures.
- ΔT_c and Glover-Rowe parameters had similar effects on the low- and intermediate-temperature cracking susceptibility. Binders with ABR levels less than 20% was at an aging level equivalent to its RTFO aged base binder and after one PAV was nearly equivalent to PAV condition of its base binder. Binders with ABR of 20% or more was tested as-is, they had values of brittleness parameter higher than their PAV aged base binder, and after one PAV aging they exceeded the values of their second-PAV-aged base binders indicating extreme stiffening effect of recycled binders.
- According to the comparison of the binder rheological data with the mix performance testing results conducted as part of the ICT R27-128 study (Al-Qadi et al. 2015), the results are consistent in terms of correlating critical rheological properties with the Illinois Flexibility Index Test (I-FIT) results.
- Results indicate that AC with high levels of ABR prepared with only RAS could have short- and long-term cracking potential. This is because aging progresses much faster in such cases, while their lifetime starts at an already-critically-aged condition. Hence, the use of RAS to produce high levels of ABR in mixes should be carefully examined prior to the use for a given application. The possibility of using proper rejuvenators or softening agents that can be blended and counter the effects of stiff binders should be investigated.

REFERENCES

AASHTO. (2014). Standard Practice for Design Considerations When Using Reclaimed Asphalt Shingles (RAS) in Asphalt Mixtures.

Abbas, A. R., Mannan, U. A., & Dessouky, S. (2013). Effect of recycled asphalt shingles on physical and chemical properties of virgin asphalt binders. *Construction and Building Materials*, *45*, 162-172.

Al-Qadi, I. L., Aurangzeb, Q., Carpenter, S. H., Pine, W. J., & Trepanier, J. (2012). Impact of high RAP contents on structural and performance properties of asphalt mixtures. *FHWA-ICT-12-002*.

Al-Qadi, I. L., Carpenter, S. H., Roberts, G., Ozer, H., Aurangzeb, Q., Elseifi, M., & Trepanier, J. (2009). *Determination of usable residual asphalt binder in RAP*. Illinois Center for Transportation (ICT).

Al-Qadi, I. L., Ozer, H., Lambros, J., El Khatib, A., Singhvi, P., Khan, T., ... & Doll, B. (2015). *Testing Protocols to Ensure Performance of High Asphalt Binder Replacement Mixes Using RAP and RAS*. Illinois Center for Transportation/Illinois Department of Transportation.

Anderson, R. M., King, G. N., Hanson, D. I., & Blankenship, P. B. (2011). Evaluation of the relationship between asphalt binder properties and non-load related cracking. *Journal of the Association of Asphalt Paving Technologists*, *80*.

Cascione, A. A., Williams, R. C., & Yu, J. (2015). Performance testing of asphalt pavements with recycled asphalt shingles from multiple field trials. *Construction and Building Materials*, *101*, 628-642.

Colbert, B., & You, Z. (2012). The properties of asphalt binder blended with variable quantities of recycled asphalt using short term and long term aging simulations. *Construction and Building Materials*, *26*(1), 552-557.

Chen, J. S., Chen, S. F., Liao, M. C., & Huang, S. W. (2014). Laboratory evaluation of asphalt blends of recycling agents mixed with aged binders. *Journal of Materials in Civil Engineering*, *27*(4), 04014143.

Cooper Jr., S. B., Mohammad, L. N., Elseifi, M. A., & Medeiros Jr, M. S. (2015). Effect of Recycling Agents on the Laboratory Performance of Asphalt Mixtures Containing Recycled Asphalt Shingles. *Transportation Research Record: Journal of the Transportation Research Board*, (2506), 54-61.

Daniel, J., Pochily, J., & Boisvert, D. (2010). Can more reclaimed asphalt pavement be added? Study of extracted binder properties from plant-produced mixtures with up to 25% reclaimed asphalt pavement. *Transportation Research Record: Journal of the Transportation Research Board*, (2180), 19-29.

Huang, S. C., Pauli, A. T., Grimes, R. W., & Turner, F. (2014). Ageing characteristics of RAP binder blends–what types of RAP binders are suitable for multiple recycling?. *Road Materials and Pavement Design*, *15*(sup1), 113-145.

Huang, S. C., & Turner, T. F. (2013). Aging Characteristics of RAP Blend Binders: Rheological Properties. *Journal of Materials in Civil Engineering*, *26*(5), 966-973.

Illinois Department of Transportation. (2015). Illinois Flexibility Index Test.

King, G., Anderson, M., Hanson, D., & Blankenship, P. (2012). Using black space diagrams to predict age-induced cracking. In *7th RILEM International Conference on Cracking in Pavements* (pp. 453-463). Springer Netherlands.

Khosla, N. P., Nair, H., Visintine, B., & Malpass, G. (2012). Effect of reclaimed asphalt and virgin binder on rheological properties of binder blends. *International Journal of Pavement Research and Technology*, *5*(5), 317-325.

Lippert, D., & Brownlee, M. (2012). *Use of reclaimed asphalt shingles in Illinois* (No. IL-PRR-162).

Liu, G., Nielsen, E., Komacka, J., Leegwater, G., & van de Ven, M. (2015). Influence of soft bitumens on the chemical and rheological properties of reclaimed polymer-modified binders from the "old" surface-layer asphalt. *Construction and Building Materials*, *79*, 129-135.

Mensching, D. J., Rowe, G. M., Daniel, J. S., & Bennert, T. (2015). Exploring low-temperature performance in Black Space. *Road Materials and Pavement Design*, *16*(sup2), 230-253.

Mogawer, W. S., Austerman, A. J., & Bonaquist, R. (2016). Using Space Diagrams to Evaluate the Effect of Softer Binder and Warm Mix Technologies in Reclaimed Asphalt Pavement Mixtures. In *Transportation Research Board 95th Annual Meeting* (No. 16-1547).

Nelson, G., Shenoy, A., Xicheng, Q., Aroon, S., Ghazi, A., Adrian, A., ... & Thomas, H. (2012). Performance testing for superpave and structural validation. (No. FHWA-HRT-11--45), 2012, pp. 276.

Ozer, H., Al-Qadi, I. L., Lambros, J., El-Khatib, A., Singhvi, P., & Doll, B. (2016). Development of the fracture-based flexibility index for asphalt concrete cracking potential using modified semi-circle bending test parameters. *Construction and Building Materials*, *115*, 390-401.

Ozer, H., Al-Qadi, I. L., Singhvi, P., Khan, T., Rivera-Perez, J., & El-Khatib, A. (2016). Fracture Characterization of Asphalt Mixtures with High Recycled Content Using Illinois Semicircular Bending Test Method and Flexibility Index. *Transportation Research Record: Journal of the Transportation Research Board*, (2575), 130-137.

Rowe, G. (2014). Analysis of SHRP Core Asphalts – New 2013/14 Test Results. Presentation from the Binder Expert Task Group Meeting, San Antonio, TX.

Rowden, L. (2013). *Utilization of Recycled and Reclaimed Materials in Illinois Highway Construction in 2012* (No. IL-PRR-164).

Solanki, P., Zaman, M., Adje, D., & Hossain, Z. (2014). Effect of recycled asphalt pavement on thermal cracking resistance of hot-mix asphalt. *International Journal of Geomechanics*, *15*(5), A4014001

Willis, J. R., & Turner, P. (2016). Characterization of Asphalt Binder Extracted from Reclaimed Asphalt Shingles.

Zhou, F., Li, H., Lee, R., Scullion, T., & Claros, G. (2013). Recycled asphalt shingle binder characterization and blending with virgin binders. *Transportation Research Record: Journal of the Transportation Research Board*, (2370), 33-43.

Zhao, S., Nahar, S. N., Schmets, A. J., Huang, B., Shu, X., & Scarpas, T. (2015). Investigation on the microstructure of recycled asphalt shingle binder and its blending with virgin bitumen. *Road Materials and Pavement Design*, *16*(sup1), 21-38.

APPENDIX

A. DSR Data Analysis Procedure

a) Data preprocessing

1. Open frequency raw data on your computer using excel.
    - You can also open the file on your own computer without install the DSR program by just enable “All Flies”. (Figure 1).

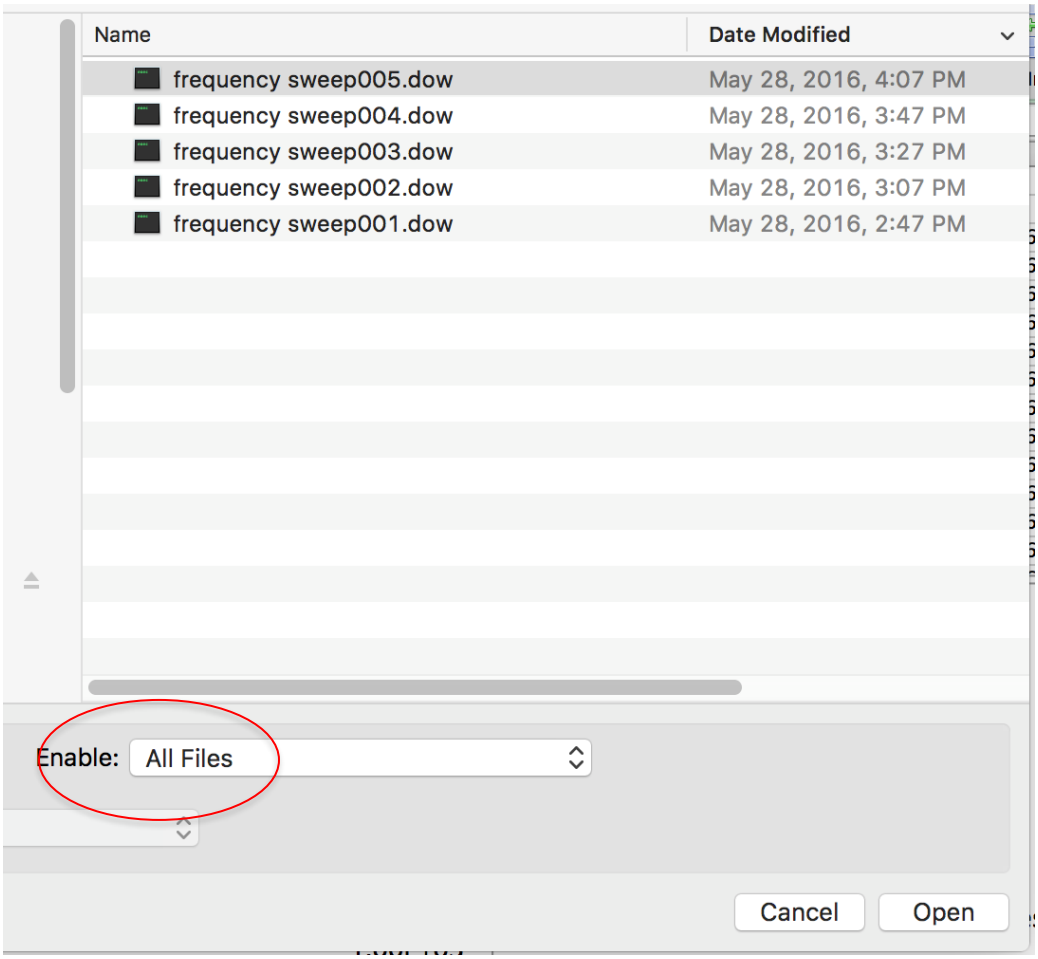

Figure A.1

- Select “Delimited”, and then “Tab” and “Comma”. (Figure 2 and Figure 3)

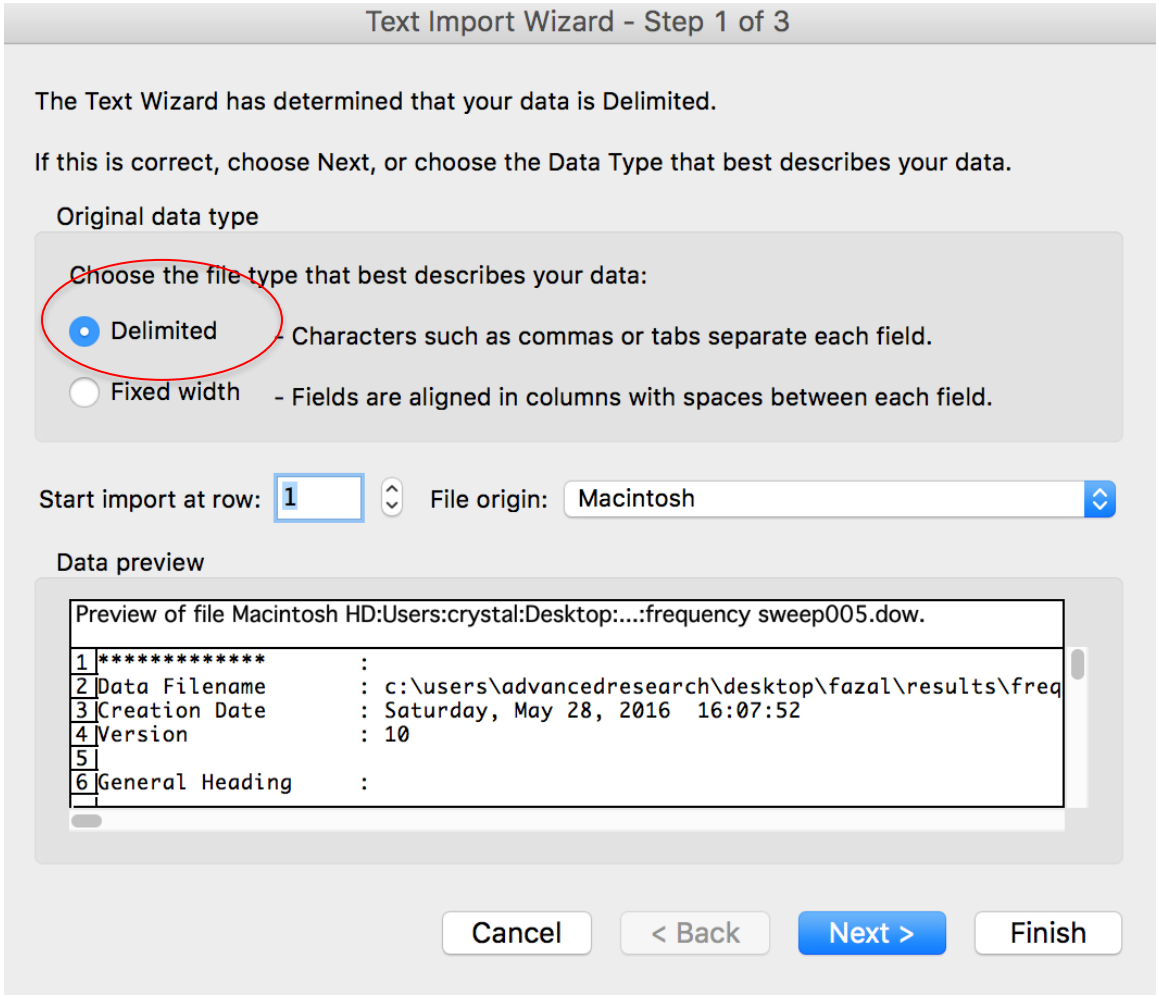

Figure A.2

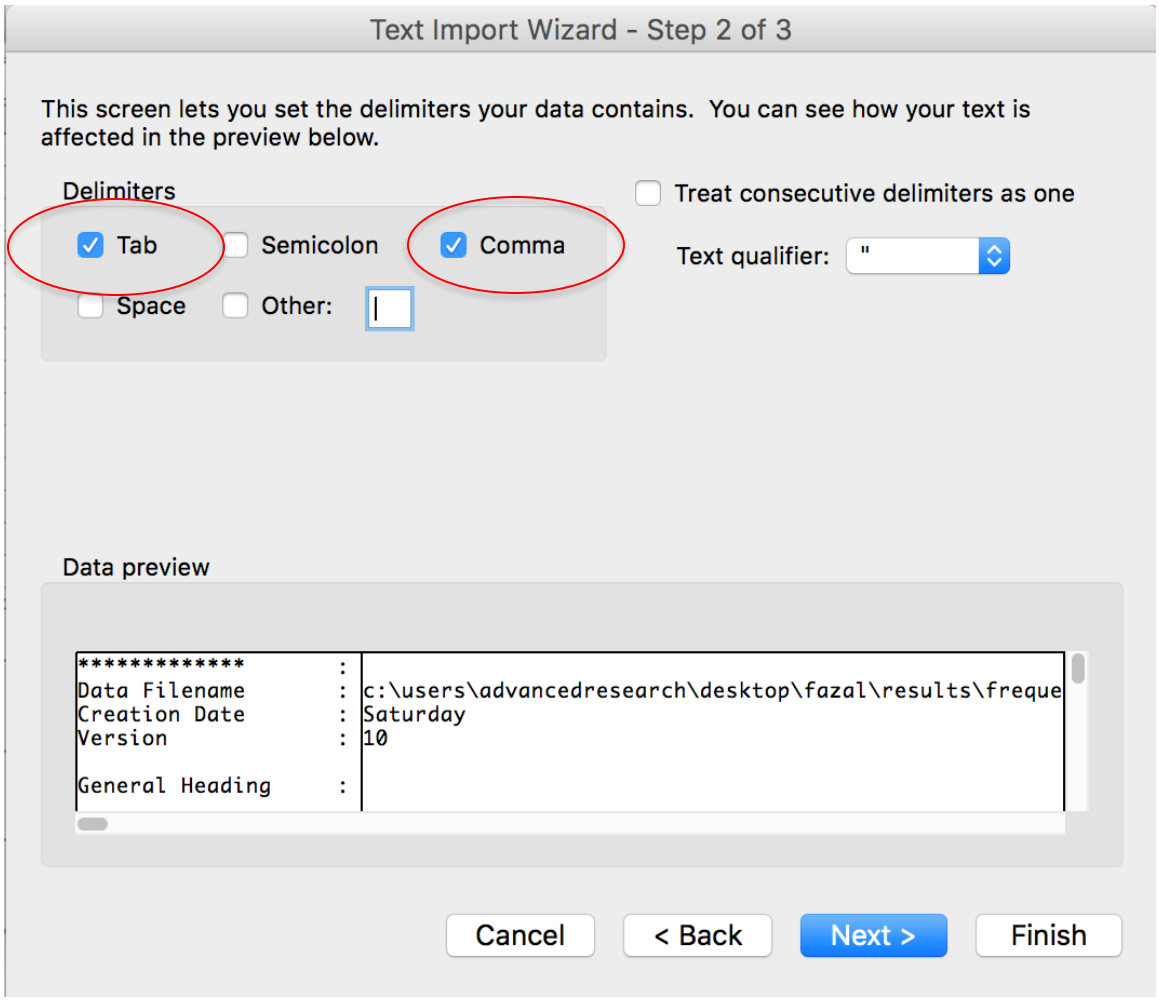
Text Import Wizard - Step 2 of 3
This screen lets you set the delimiters your data contains. You can see how your text is affected in the preview below.
Delimiters
Tab
Semicolon
Comma
Space
Other:
Treat consecutive delimiters as one
Text qualifier:
"
Data preview
********** :
Data Filename : c:\users\advancedresearch\desktop\fazal\results\freque
Creation Date : Saturday
Version : 10
General Heading :
Cancel
< Back
Next >
Finish

Figure A.3

2. Copy raw data in the open files and paste them into the excel for master curve shifting

- After opening the raw data. The following four columns can be found in each file (Figure 4). These data needs to be pasted into the master curve shift excel file.

	Temperature (∞C)	Frequency (Hz)	Phase Angle (∞)	Complex Mo (Pa)	Elastic Modu (Pa)	Viscous Mod (Pa)	Complex Visc (Pas)	Shear Stress (Pa)	Strain ( )	Thrust (g)
3	40.01	1.00E-01	84.95	1.95E+03	1.72E+02	1.94E+03	3.11E+03	1.92E+01	9.86E-03	6.60E-02
7	40.05	1.19E-01	84.57	2.28E+03	2.16E+02	2.27E+03	3.06E+03	2.24E+01	9.79E-03	0.4
7	40.02	1.41E-01	84.24	2.69E+03	2.70E+02	2.67E+03	3.03E+03	2.62E+01	9.76E-03	0.3
8	40.03	1.68E-01	83.98	3.16E+03	3.31E+02	3.14E+03	2.99E+03	3.09E+01	9.78E-03	0.3
1	40.09	2.00E-01	83.84	3.69E+03	3.96E+02	3.67E+03	2.94E+03	3.62E+01	9.82E-03	8.80E-02
9	39.95	2.37E-01	83.4	4.34E+03	4.99E+02	4.31E+03	2.91E+03	4.25E+01	9.80E-03	0.1
7	40.01	2.82E-01	83.04	5.11E+03	6.18E+02	5.07E+03	2.88E+03	5.01E+01	9.81E-03	0.2
7	39.99	3.35E-01	82.68	5.97E+03	7.61E+02	5.92E+03	2.84E+03	5.85E+01	9.80E-03	0.2
4	40.02	3.98E-01	82.32	7.00E+03	9.36E+02	6.94E+03	2.80E+03	6.85E+01	9.79E-03	0.2
5	39.93	4.73E-01	81.99	8.22E+03	1.15E+03	8.14E+03	2.77E+03	8.06E+01	9.80E-03	0.3
6	40.04	5.62E-01	81.55	9.55E+03	1.40E+03	9.45E+03	2.70E+03	9.36E+01	9.80E-03	0.5
7	40.03	6.68E-01	81.19	1.12E+04	1.71E+03	1.10E+04	2.66E+03	1.09E+02	9.78E-03	0.1
6	39.93	7.94E-01	80.87	1.31E+04	2.08E+03	1.29E+04	2.62E+03	1.29E+02	9.84E-03	-2.90E-02
5	39.93	9.44E-01	80.35	1.53E+04	2.57E+03	1.51E+04	2.58E+03	1.50E+02	9.81E-03	0.3

Figure A.4

- Paste the four columns data correctly into the master curve shift excel file (Figure 5). Each temperature should be changed to be **constant** and paste the high temperature test data first then low. For example, if your test temperatures are 50,40,30 and 20, paste 50 first then 40 then 30 finally 20.

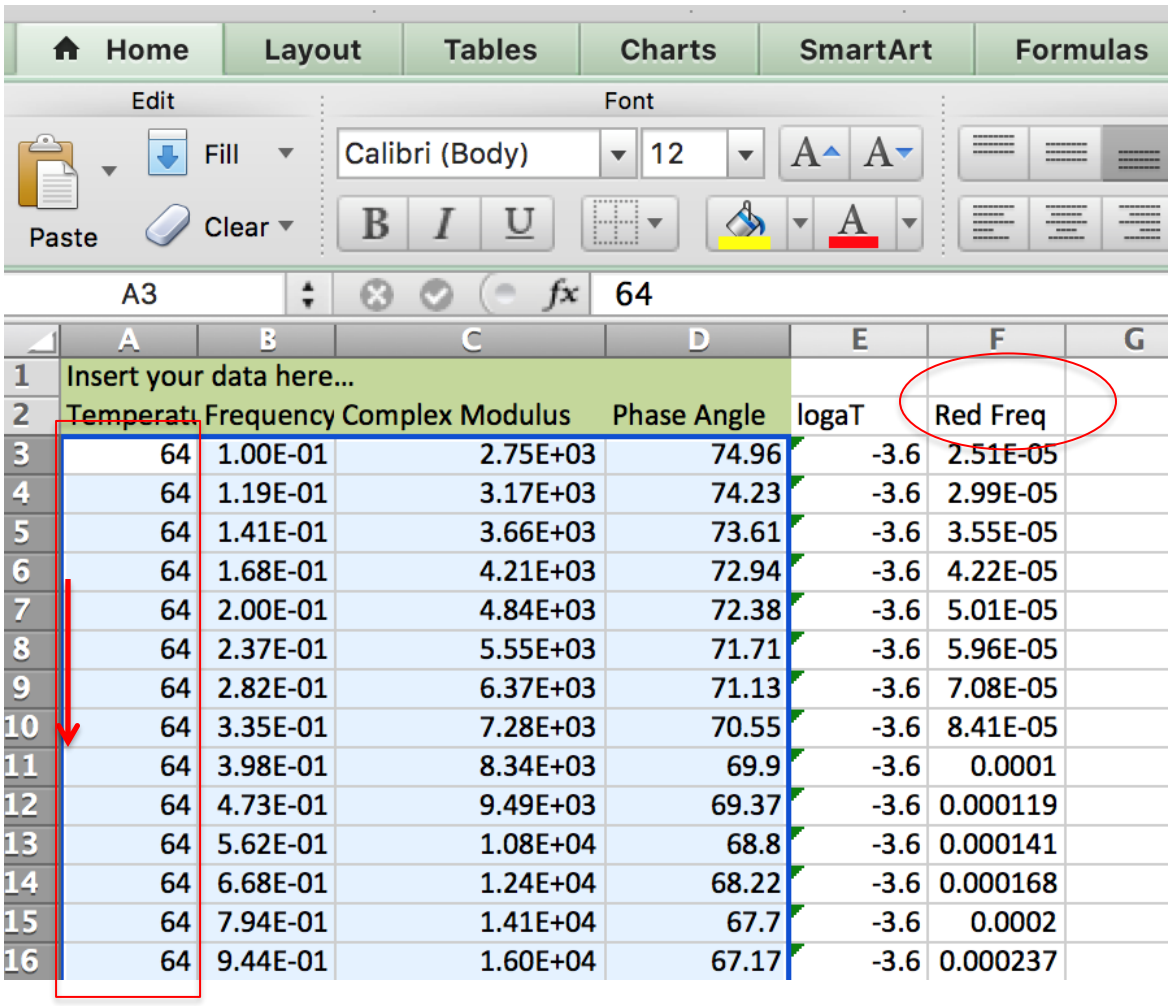

	A	B	C	D	E	F	G
1	Insert your data here...						
2	Temperatu	Frequency	Complex Modulus	Phase Angle	logaT	Red Freq	
3	64	1.00E-01	2.75E+03	74.96	-3.6	2.51E-05	
4	64	1.19E-01	3.17E+03	74.23	-3.6	2.99E-05	
5	64	1.41E-01	3.66E+03	73.61	-3.6	3.55E-05	
6	64	1.68E-01	4.21E+03	72.94	-3.6	4.22E-05	
7	64	2.00E-01	4.84E+03	72.38	-3.6	5.01E-05	
8	64	2.37E-01	5.55E+03	71.71	-3.6	5.96E-05	
9	64	2.82E-01	6.37E+03	71.13	-3.6	7.08E-05	
10	64	3.35E-01	7.28E+03	70.55	-3.6	8.41E-05	
11	64	3.98E-01	8.34E+03	69.9	-3.6	0.0001	
12	64	4.73E-01	9.49E+03	69.37	-3.6	0.000119	
13	64	5.62E-01	1.08E+04	68.8	-3.6	0.000141	
14	64	6.68E-01	1.24E+04	68.22	-3.6	0.000168	
15	64	7.94E-01	1.41E+04	67.7	-3.6	0.0002	
16	64	9.44E-01	1.60E+04	67.17	-3.6	0.000237	

Figure A.5

3. Plot and shift master curve

- After you paste the data you can plot the complex modulus (column C) versus reduced frequency (column F) (Figure 5) as showing in the Figure 6 (before shifting).

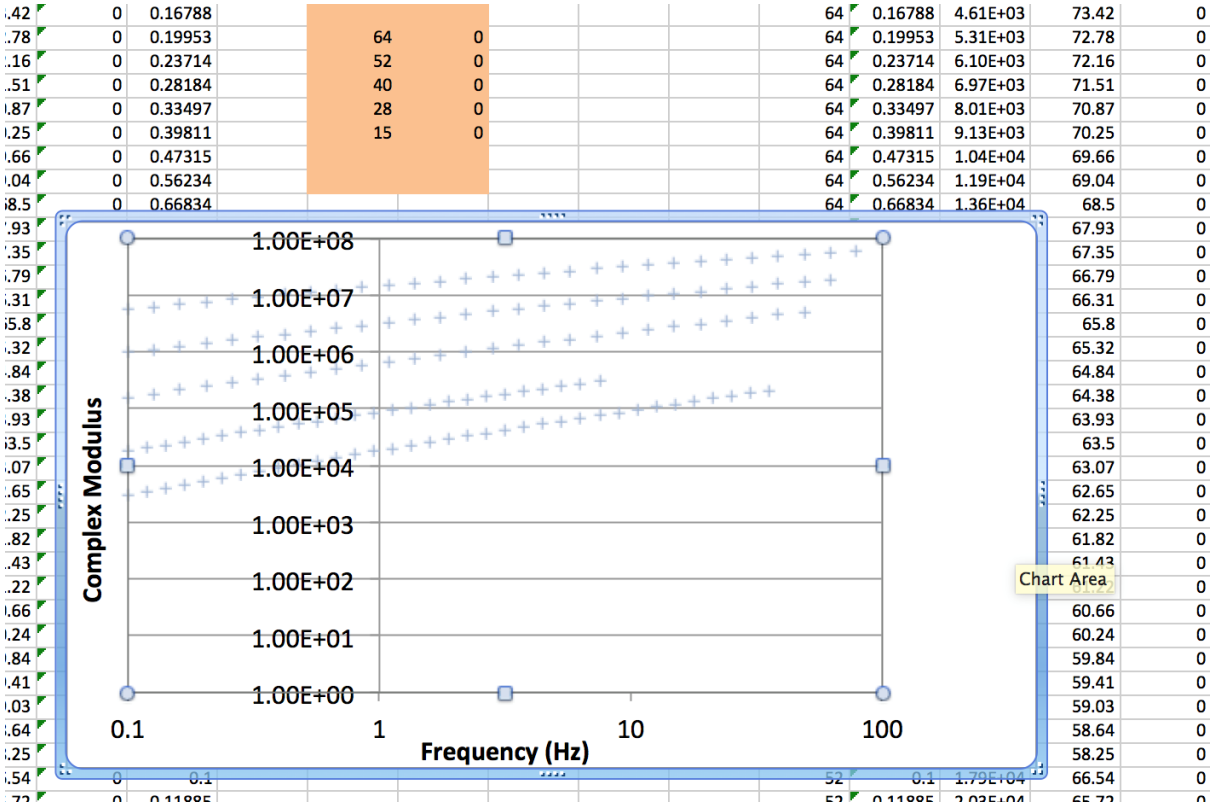

Figure A.6

- Insert your test temperature following the excel note. Adjust the shift factor (log aT) to shift the master curves (Figure 7). The algorithm of the shifting was introduced in chapter 2. The shifted master curve is shown as in Figure7.

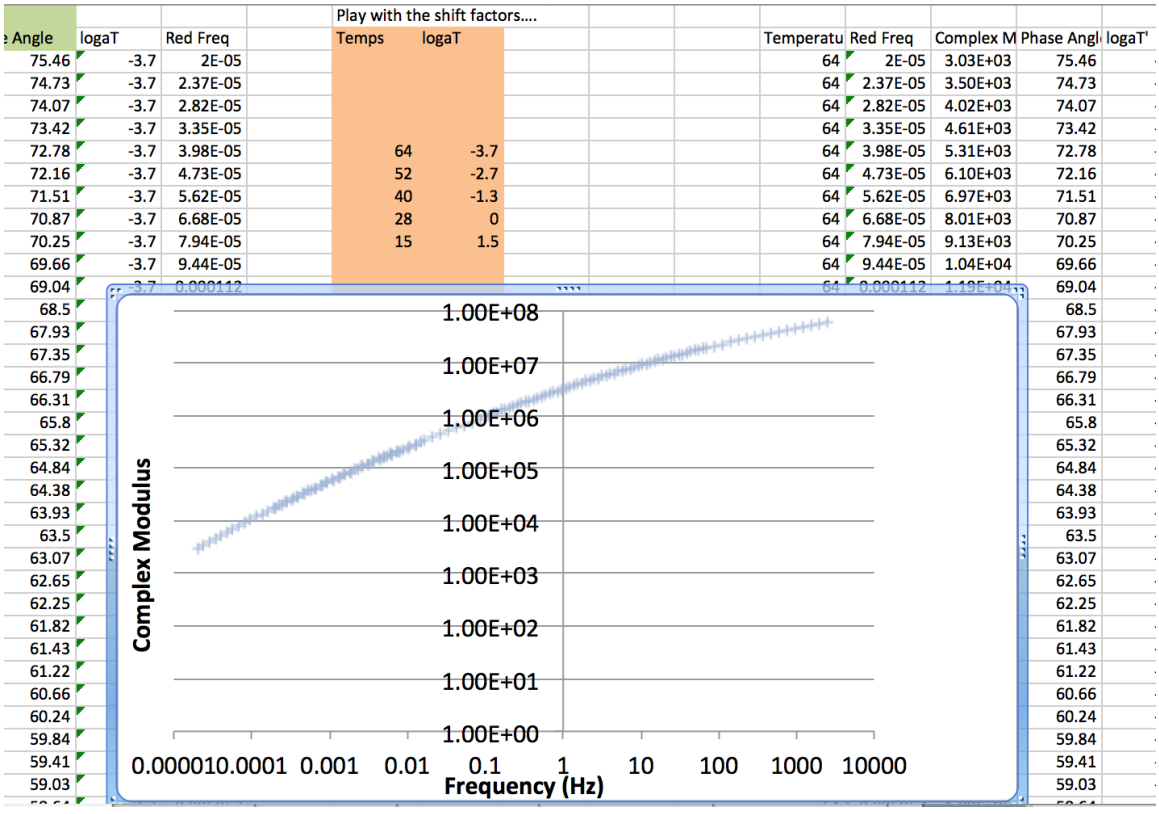

Figure A.7

4. Remove inconsistent data

- There might be some inconsistent data that need to be removed. Thus you need to check the plot of phase angle (column D) versus reduced frequency (column F) showed in Figure 5. Garbage data in the phase angle plot is shown in Figure 8:

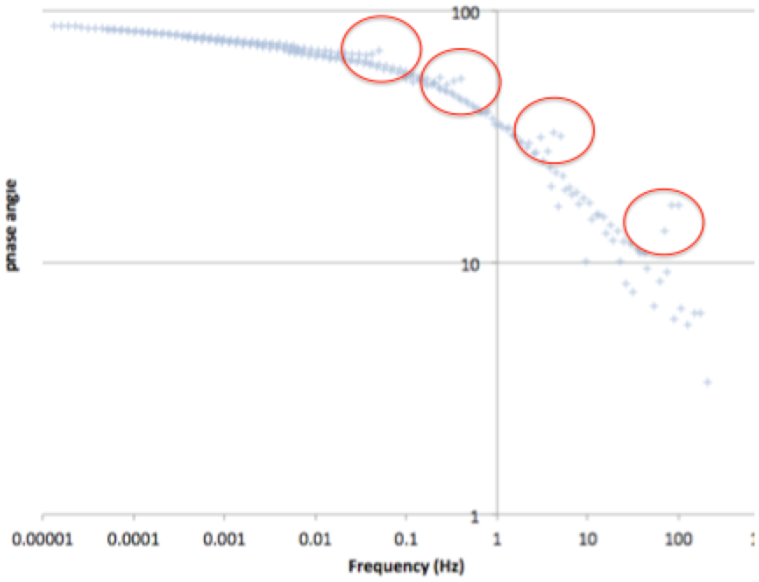

Figure A.8

5. Move fitted and cleaned data and sort them

- Copy columns MNOPQ and paste to columns STUVW (Figure 9). Sort column T (frequency) from **low to high**. Then the data of columns STUVW need to be saved to a txt file.

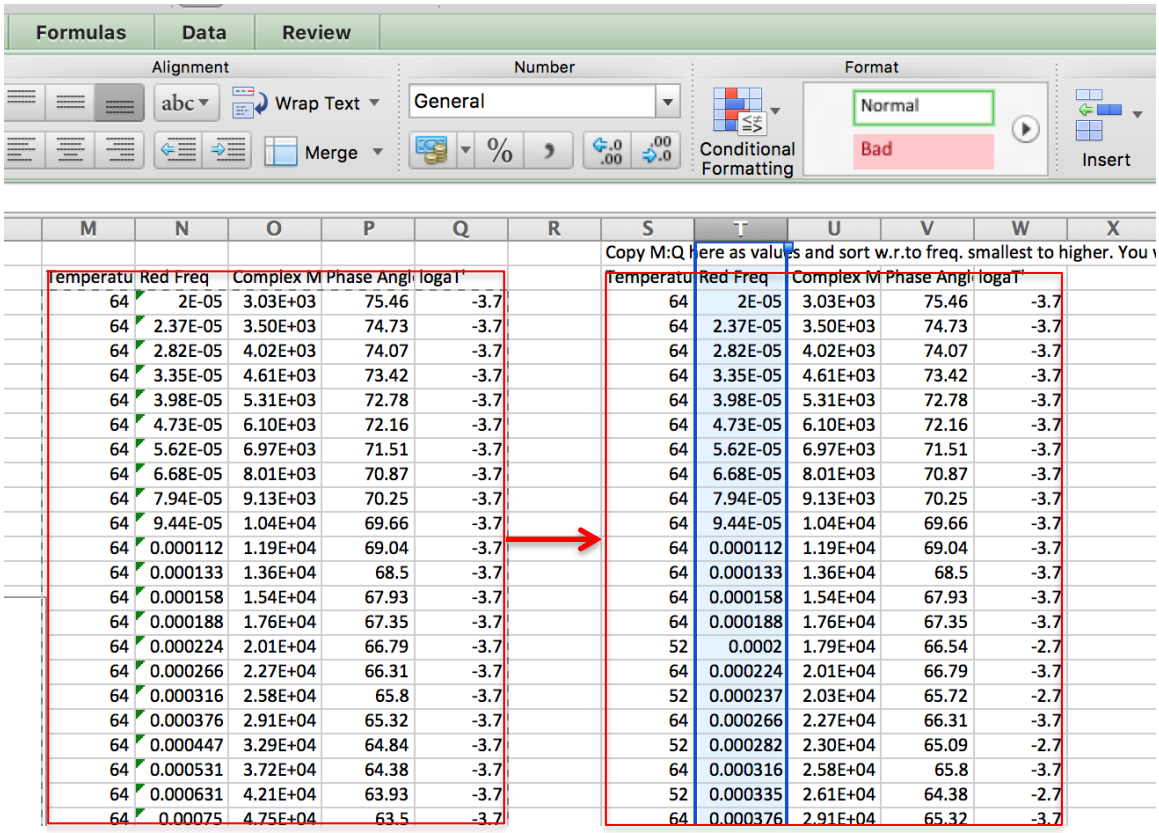

Figure A.9

6. Save preprocessed data as a txt file

- The txt file is shown in Figure 10. Except the data from columns STUVW, you need add the number of temperatures, which are your test temperatures.

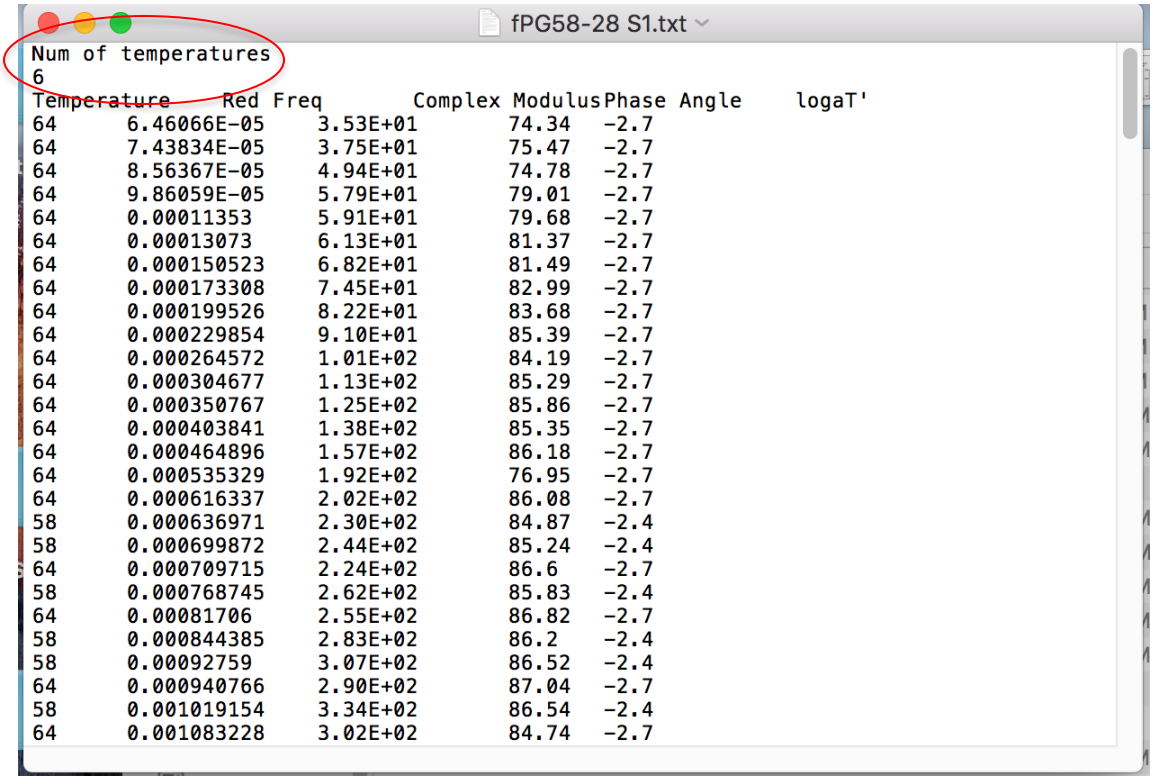

Figure A.10

b) MATLAB Master Curve Sigmoidal Model Fit

Run the master curve shift MATLAB program. Input your txt file and choose sigmoidal fit. Follow the instructions, then the output file from MATLAB program is like shown in Figure 11, and find these data paste them into the excel for rheology parameter calculation (GR, crossover frequency and R-value).

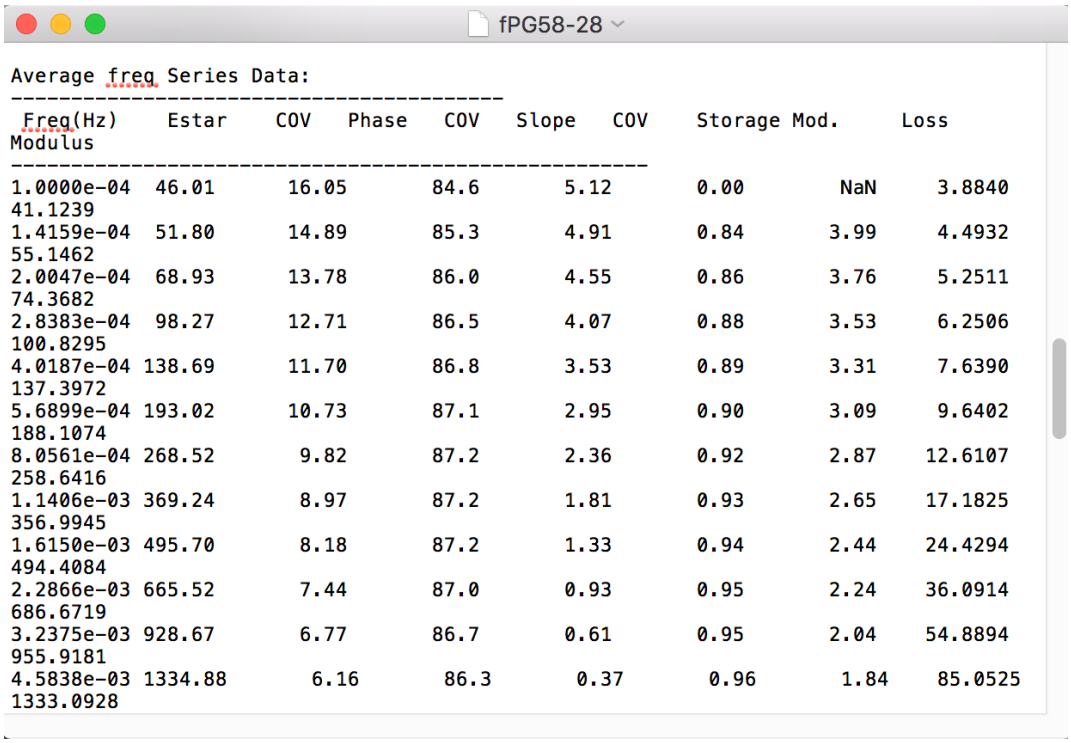

Figure A.11

c) Rheology Parameters Calculation

1. Input data into excel for MATLAB read

- The Excel for rheology calculation is shown in Figure 12. The column A and B are your test temperature and shift factors, the same for CD because here we have two test replicates. If you only have one replicate, please make CD is same as AB. The column EF are prony series coefficients, you also can find it in the MATLAB output file.
- Make sure paste everything at the correct location, otherwise the program cannot give the correct answer.

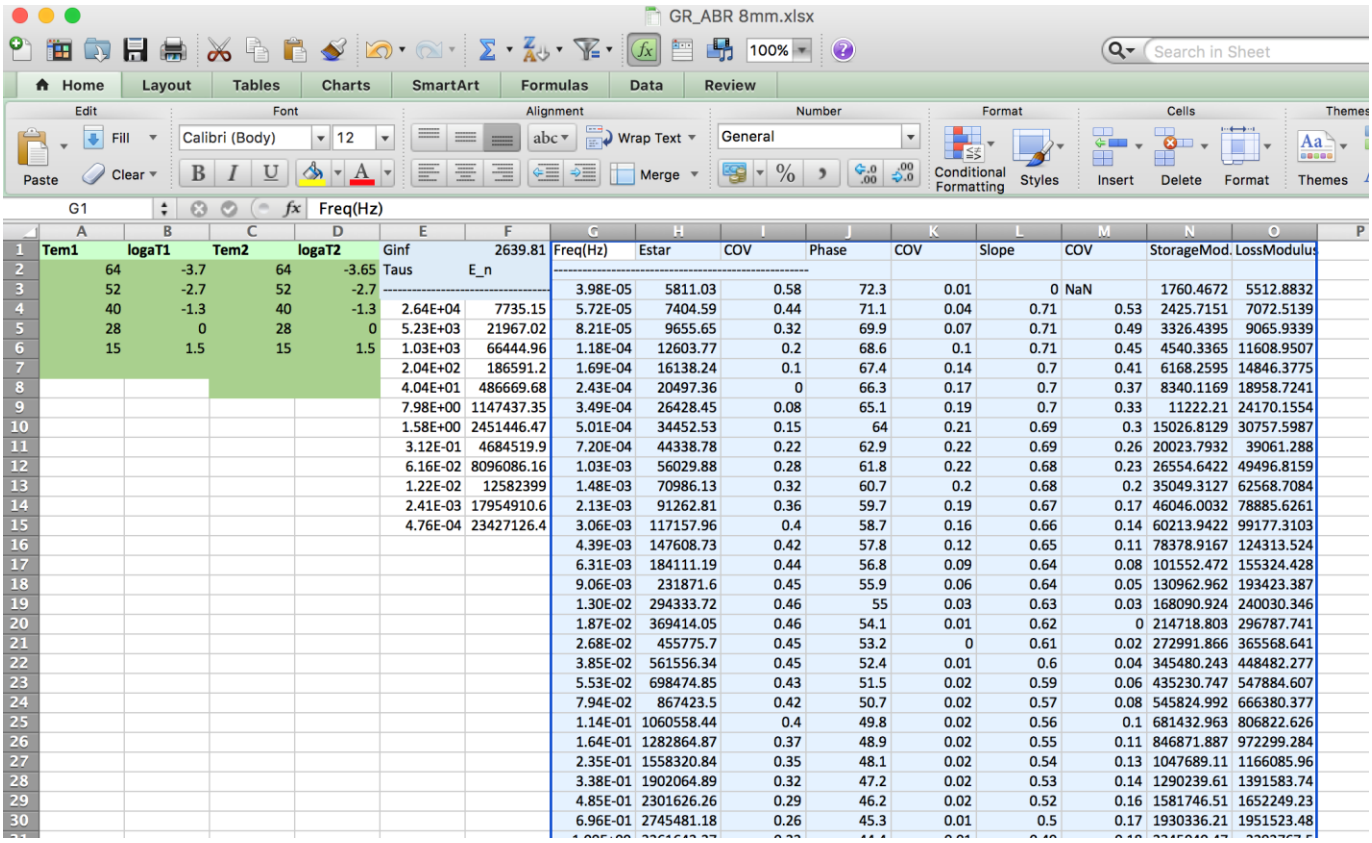

	A	B	C	D	E	F	G	H	I	J	K	L	M	N	O
1	Tem1	logaT1	Tem2	logaT2	Ginf	2639.81	Freq(Hz)	Estar	COV	Phase	COV	Slope	COV	StorageMod.	LossModulus
2	64	-3.7	64	-3.65	Taus	E_n	----------								
3	52	-2.7	52	-2.7	----------		3.98E-05	5811.03	0.58	72.3	0.01	0	NaN	1760.4672	5512.8832
4	40	-1.3	40	-1.3	2.64E+04	7735.15	5.72E-05	7404.59	0.44	71.1	0.04	0.71	0.53	2425.7151	7072.5139
5	28	0	28	0	5.23E+03	21967.02	8.21E-05	9655.65	0.32	69.9	0.07	0.71	0.49	3326.4395	9065.9339
6	15	1.5	15	1.5	1.03E+03	66444.96	1.18E-04	12603.77	0.2	68.6	0.1	0.71	0.45	4540.3365	11608.9507
7					2.04E+02	186591.2	1.69E-04	16138.24	0.1	67.4	0.14	0.7	0.41	6168.2595	14846.3775
8					4.04E+01	486669.68	2.43E-04	20497.36	0	66.3	0.17	0.7	0.37	8340.1169	18958.7241
9					7.98E+00	1147437.35	3.49E-04	26428.45	0.08	65.1	0.19	0.7	0.33	11222.21	24170.1554
10					1.58E+00	2451446.47	5.01E-04	34452.53	0.15	64	0.21	0.69	0.3	15026.8129	30757.5987
11					3.12E-01	4684519.9	7.20E-04	44338.78	0.22	62.9	0.22	0.69	0.26	20023.7932	39061.288
12					6.16E-02	8096086.16	1.03E-03	56029.88	0.28	61.8	0.22	0.68	0.23	26554.6422	49496.8159
13					1.22E-02	12582399	1.48E-03	70986.13	0.32	60.7	0.2	0.68	0.2	35049.3127	62568.7084
14					2.41E-03	17954910.6	2.13E-03	91262.81	0.36	59.7	0.19	0.67	0.17	46046.0032	78885.6261
15					4.76E-04	23427126.4	3.06E-03	117157.96	0.4	58.7	0.16	0.66	0.14	60213.9422	99177.3103
16							4.39E-03	147608.73	0.42	57.8	0.12	0.65	0.11	78378.9167	124313.524
17							6.31E-03	184111.19	0.44	56.8	0.09	0.64	0.08	101552.472	155324.428
18							9.06E-03	231871.6	0.45	55.9	0.06	0.64	0.05	130962.962	193423.387
19							1.30E-02	294333.72	0.46	55	0.03	0.63	0.03	168090.924	240030.346
20							1.87E-02	369414.05	0.46	54.1	0.01	0.62	0	214718.803	296787.741
21							2.68E-02	455775.7	0.45	53.2	0	0.61	0.02	272991.866	365568.641
22							3.85E-02	561556.34	0.45	52.4	0.01	0.6	0.04	345480.243	448482.277
23							5.53E-02	698474.85	0.43	51.5	0.02	0.59	0.06	435230.747	547884.607
24							7.94E-02	867423.5	0.42	50.7	0.02	0.57	0.08	545824.992	666380.377
25							1.14E-01	1060558.44	0.4	49.8	0.02	0.56	0.1	681432.963	806822.626
26							1.64E-01	1282864.87	0.37	48.9	0.02	0.55	0.11	846871.887	972299.284
27							2.35E-01	1558320.84	0.35	48.1	0.02	0.54	0.13	1047689.11	1166085.96
28							3.38E-01	1902064.89	0.32	47.2	0.02	0.53	0.14	1290239.61	1391583.74
29							4.85E-01	2301626.26	0.29	46.2	0.02	0.52	0.16	1581746.51	1652249.23
30							6.96E-01	2745481.18	0.26	45.3	0.01	0.5	0.17	1930336.21	1951523.48

Figure A.12

2. Run the MATLAB program

- Run Rheology_index_calculation.m, input your excel file name (line14 in Figure 13) and your number of sheet (line 20 in Figure 13)

```
10
11      % ----   input filename and number of binders -----  %
12
13      % insert your filename here, the file contains your data
14 -    filename = 'GR_ABR 8mm.xlsx';
15
16      % insert your number of sheet in the file
17      % each sheet corresponding one type of binder
18      % for example here: 20 sheet correponding to 20 binders
19
20 -    number_of_sheet = 20;
21
22
```

Figure A.13

- Input your reference temperature of your master curve (line 38 in Figure 14)
- Input the rheology index required frequency and temperature (line 47 and 49 in Figure 14). An example shown in line 41.

```
35      % ------ input data --------- %
36
37      % *** input your reference temperatrue ***
38 -    ref_t = 28;
39
40      % *** input your frequency and temperature of each parameter ***
41      % for example here:
42      % @GR: frequency 0.005 rad/s and temperature 15C
43      %           thus w[1] = 0.005 ; T[1] = 15
44      % @rutting: frequency 10rad/s and temperature 50C
45      %           thus w[2] = 10; T[2] = 50
46
47 -    w = [0.005;10];                              %unit rad/s
48
49 -    T = [15;50];
50
```

Figure A.14

- Figure 15 shows the input modulus and phase angle of GR parameter and rutting parameter. You don't need to make any change here, just to remind, because we input w[1] and T[1] for GR calculation, thus here G_gr (line85) is gstar2(1) and phase_angle_gr (line 87) is phase_angle(1); and we input w[2] and T[2] for rutting calculation, thus here G_rutting is gstar2(2) and phase_angle _rutting is phase_angle(2).

```
82    %% Glover-Rowe Parameter calculation
83
84    %insert the complex modulus used to calculate the GR parameter
85 -  G_gr = gstar2(1);                                              %unit Pa
86    %insert the phase angle used to calculate the GR parameter
87 -  phase_angle_gr = phase_angle(1);                               %unit deg
88
89
90 -  GR{i} = GR_calculation(G_gr,phase_angle_gr);                    %unit Pa
91
92    %% Rutting Parameter calculation
93
94    %insert the complex modulus used to calculate the rutting parameter
95 -  G_rutting = gstar2(2);                                          %unit Pa
96
97    %insert the phase angle used to calculate the rutting parameter
98 -  phase_angle_rutting = phase_angle(2);                          %unit deg
99
100
101 -  rutting{i} = Rutting_calculation(G_rutting,phase_angle_rutting);   %unit Pa
102
```

Figure A.15

- There is some commented code in the complex modulus and phase angle calculation part, you can also uncomment them to plot the figure of complex modulus and phase angle like Figure 16 and 17, to check the points used to calculate GR and rutting parameter are at a correct place.

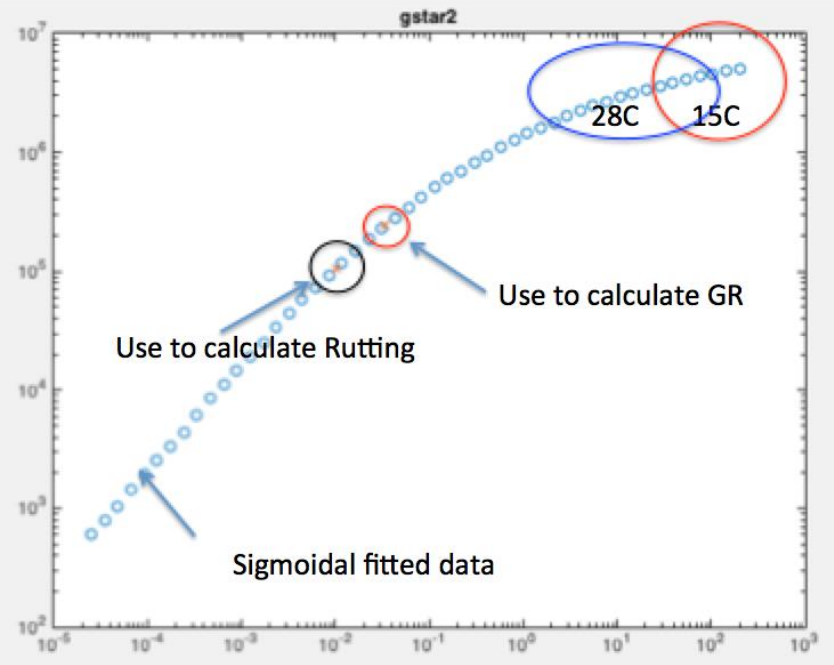

Figure A.16

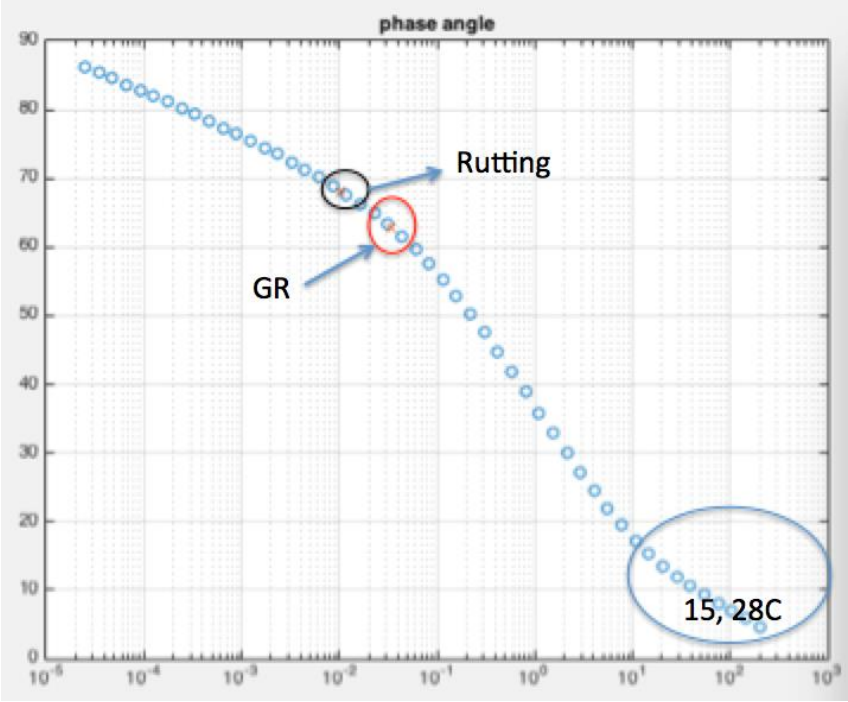

Figure A.17

3. Read table

- Finally the MATLAB program will give you a such table about all the calculation results.

number	Glover_Rowe_Pa	Rutting_Pa	crossover_frequency_Hz	R_value
1	65.022	6263.4	12728	0.59307
2	661.8	13115	11488	0.46596
3	922.09	21628	9392	0.85435
4	6770.7	38642	2403	1.2104
5	23645	67057	311.86	1.7333
6	1.069e+05	1.4714e+05	123.36	1.5755
7	2.0769e+05	1.6136e+05	27.528	1.8662
8	7.5765e+05	3.4341e+05	8.4551	1.7398
9	8665.1	46570	1167.6	1.3626
10	10099	41179	899.31	1.4635
11	93492	76234	322.54	1.7358
12	90198	1.3747e+05	168.02	1.6433
13	2.8405e+05	1.7723e+05	16.806	1.9946
14	1.1603e+05	1.2964e+05	191.62	1.5068
15	1.8712e+05	1.7297e+05	78.302	1.6799
16	2.4369e+05	2.4587e+05	13.946	1.9635
17	2.8088e+05	2.3597e+05	20.663	1.8228
18	1.2699e+06	3.9026e+05	0.54255	2.3359
19	8.7553e+05	5.0029e+05	15.865	1.5253
20	73975	1.0687e+05	217.98	1.5677

Figure A.18

B. MATLAB Code of Rheology Index Calculation

a) Main Program

```
% Developed by Jing Ma 2015
% jingma6@illinois.edu
% This small program is used to calculate Glover-Rowe parameter, Rutting parameter, R-value and
% crossover frequency.
% also can be used for calculate other performance index once you input the
% required information.
%-------------------------------------------------------------------------%

clc;clear;close all;

% ----   input filename and number of binders -----  %

% insert your filename here, the file contains your data
filename = 'GR_ABR 8mm.xlsx';

% insert your number of sheet in the file
% each sheet corresponding one type of binder
% for example here: 20 sheet correponding to 20 binders

number_of_sheet = 20;


% ------   read file   --------%
for i = 1:number_of_sheet;
    sheet = i;
wlf1 = xlsread(filename,sheet,'A2:B17');    %read WLF of sample1
wlf2 = xlsread(filename,sheet,'C2:D17');    %read WLF of sample2
G_inf = xlsread(filename,sheet,'F1:F1');    %read prony series
E_n = xlsread(filename,sheet,'F4:F20');     %read prony series
taus = xlsread(filename,sheet,'E4:E20');    %read prony series
fre = xlsread(filename,sheet,'G3:G52');     %read reduced frequency, unit Hz
phase = xlsread(filename,sheet,'J3:J52');   %read phase angle, unit deg
E_star = xlsread(filename,sheet,'H3:H52');  %read complex modulus, unit pa

% ------ input data --------- %

% *** input your reference temperatrue ***
ref_t = 28;

% *** input your frequency and temperature of each parameter ***
% for example here:
% @GR: frequency 0.005 rad/s and temperature 15C
%          thus w[1] = 0.005 ; T[1] = 15
% @rutting: frequency 10rad/s and temperature 50C
%          thus w[2] = 10; T[2] = 50

w = [0.005;10];                         %unit rad/s
```

```
T = [15;50];


%% WLF fitted reduced frequency
[wr] = fitted_wr(wlf1,wlf2,T,ref_t,w);              %% rad/s
wrHz = wr.* 0.15915494327;                           %% rad/s to Hz

%% Prony fitted Complex modulus (some issues here, calculations are not based on these data)
gstar1 = Pronyfit(wrHz,G_inf,E_n,taus);


%% Interpolate Sigmoidal fitted complex modulus and phase angle

%complex modulus
gstar2 = spline(fre,E_star,wrHz);

%(here you can un-comment the figure and check if the calculation is right
%or nor)

%figure;
%loglog(x,E_star,'o',wrHz,gstar2,'x');
%title('gstar2');

% phase angle
phase_angle = spline(fre,phase,wrHz);

%(here you can un-comment the figure and check if the calculation is right
%or nor)

%figure;
%semilogx(x,y,'o',xx,phase_angle,'x');
%title('phase angle');

%% Glover-Rowe Parameter calculation

%insert the complex modulus used to calculate the GR parameter
G_gr = gstar2(1);                                    %unit Pa
%insert the phase angle used to calculate the GR parameter
phase_angle_gr = phase_angle(1);                     %unit deg


GR{i} = GR_calculation(G_gr,phase_angle_gr);                  %unit Pa

%% Rutting Parameter calculation

%insert the complex modulus used to calculate the rutting parameter
G_rutting = gstar2(2);                               %unit Pa

%insert the phase angle used to calculate the rutting parameter
phase_angle_rutting = phase_angle(2);                %unit deg
```

```
rutting{i} = Rutting_calculation(G_rutting,phase_angle_rutting);   %unit Pa

%% Crossover frequency calculation

crossover_frequency{i} = wc_calculation(fre,phase,wlf1,wlf2,ref_t);

%% R-value calculation
R_value{i} = R_value_calculation(fre,E_star,crossover_frequency{i});
end

%table generation
number = [1:number_of_sheet]';
Glover_Rowe_Pa = cell2mat(GR)';
Rutting_Pa = cell2mat(rutting)';
crossover_frequency_Hz = cell2mat(crossover_frequency)';
R_value = cell2mat(R_value)';
T = table(number,Glover_Rowe_Pa,Rutting_Pa,crossover_frequency_Hz,R_value)
```

b) Helper function called by main program

```
%this calculation based on WLF Fit (thesis chapter 2)
%@wlf1:input wlf coefficients of replicate 1
%@wlf2:input wlf coefficients of replicate 1
%@ref_t: reference temperature
%@T: the temperature you want to shift to
%@w: the reduced frequency at current reference temperature

function [wr] = fitted_wr(wlf1,wlf2,T,ref_t,w)
%% fit C1 C2
xdata1 = wlf1(:,1);
ydata1 = wlf1(:,2);
fun = @(c,xdata1)-c(1)*(xdata1 - ref_t)./(c(2)+xdata1-ref_t);
c0=[19,92];
c1 = lsqcurvefit(fun,c0,xdata1,ydata1);
xdata2 = wlf2(:,1);
ydata2 = wlf2(:,2);
fun = @(c,xdata2)-c(1)*(xdata2 - ref_t)./(c(2)+xdata2-ref_t);
c2 = lsqcurvefit(fun,c0,xdata2,ydata2);

%% logat and wr
logat1= -c1(1)*(T - ref_t)./(c1(2)+T-ref_t);
logat2= -c2(1)*(T - ref_t)./(c2(2)+T-ref_t);
wr1 = 10.^(log10(w.*0.15915494327)+logat1)./0.15915494327;    %%rad/s
wr2 = 10.^(log10(w.*0.15915494327)+logat2)./0.15915494327;
wr = (wr1+wr2)./2;                                  %%rad/s
end

function [gstar1] = Pronyfit(wrHz,G_inf,E_n,taus)
for i=1:size(wrHz,1)
   n = wrHz(i);                                  %%rad/s
   g_storage(i) = G_inf + sum(E_n*n^2.*(taus.^2)./(n^2.*(taus.^2)+1));
   g_loss(i) = sum(E_n*n.* taus./((n^2).*(taus.^2)+1));
```

```
end
  gstar1 = (g_storage.^2 + g_loss.^2).^ 0.5;
%figure;
%x = fre;                              %%Hz
%loglog(x,E_star,'o',wrHz,gstar1,'x');
%title('gstar1');
end

function GR = GR_calculation(Gstar,phase_angle)
GR = Gstar*(cos(phase_angle/180*pi())^2)/sin(phase_angle/180*pi());  %PA
end

function rutting = Rutting_calculation(Gstar,phase_angle)
rutting = Gstar*sin(phase_angle/180*pi());
end

%@fre, @phase is the frequency and phase angle used to interpolate frequency at
%phase angle equals 45 degree
%@wlf1,@wlf2,@ref_T is the same input of function fitted_wr, because here
%will call the fitted_wr to shift the interpolated frequency at the
%reference temperature to 15C

function crossover_frequency = wc_calculation(fre,phase,wlf1,wlf2,ref_t)
%y1 = nonduplicate(y);
wcHz = interp1(nonduplicate(phase),fre,45) ;        %% Hz
wc = wcHz/0.15915494327;                          %% Hz to rad/s
%shift to 15C
wc_15 = fitted_wr(wlf1,wlf2,15,ref_t,wc);          %% rad/s
crossover_frequency = wc_15 * 0.15915494327;        %% Hz
end

function R_value = R_value_calculation(fre,E_star,crossover_frequency)
g = spline(fre,E_star,crossover_frequency);
syms r
Rvalue = solve(10^(9-r)== g);
R_value = eval(Rvalue);
end
```